Multiscale scattering in nonlinear Kerr-type media

Roland Maier, Barbara Verfürth

KARLSRUHE INSTITUTE OF TECHNOLOGY

CRC 1173

Participating universities

Universität Stuttgart

EBERHARD KARLS
UNIVERSITÄT
TÜBINGEN

TU
WIEN

Funded by

DFG

MULTISCALE SCATTERING IN NONLINEAR KERR-TYPE MEDIA

ROLAND MAIER[†], BARBARA VERFÜRTH[‡],

ABSTRACT. We propose a multiscale approach for a nonlinear Helmholtz problem with possible oscillations in the Kerr coefficient, the refractive index, and the diffusion coefficient. The method does not rely on structural assumptions on the coefficients and combines the multiscale technique known as Localized Orthogonal Decomposition with an adaptive iterative approximation of the nonlinearity. We rigorously analyze the method in terms of well-posedness and convergence properties based on suitable assumptions on the initial data and the discretization parameters. Numerical examples illustrate the theoretical error estimates and underline the practicability of the approach.

Key words. Helmholtz equation, nonlinear, Kerr medium, multiscale method, a priori estimates

AMS subject classifications. 65N12, **65N30**, **35G30**

1. INTRODUCTION

Wave propagation in heterogeneous and nonlinear media has arisen growing interest in the last years since corresponding materials can produce unusual effects, such as a negative refractive indices [SPW04], cloaking [PSS06], or optical bistability [GG84], to name a few. Due to the resulting new effects, the deviations from the standard setup of homogeneous, linear materials come with a wide range of applications, such as perfect lenses [Pen00] or mode-locking lasers [PWW93]. Heterogeneous materials occur, for instance, in the large field of metamaterials, i.e., artificially constructed composites [JJWM08]. Nonlinear material laws are required for instance for large intensities, when linearized models are no longer accurate enough. One important example for acoustic and electromagnetic waves are Kerr-type media [Ker75], where in general the material quantity σ depends on the wave field u like $\sigma(u) = (\sigma_0 + \sigma_2|u|^2)$. For instance, u may represent the electric field and σ the electric permittivity in electromagnetics or u may represent the pressure and σ the refractive index in acoustics.

In the time-harmonic regime, such material models often lead to the nonlinear Helmholtz equation

$$-\mathrm{div}A\nabla u - k^2 n(1 + \varepsilon\mathbb{1}_{D_\varepsilon}|u|^2)u = f,$$

where D_ε is the subdomain where the nonlinear Kerr-type medium is active, A, n, and ε are material coefficients and k is the wave number. Assumptions on these coefficients as well as appropriate boundary conditions are given further below. In this contribution, the coefficients A, n, ε may vary on small spatial scales. The nonlinear Helmholtz equation has been studied analytically and numerically for constant coefficients in [EW14, YL17, WZ18] and in layered media in [BFT09, XB10]. However, the standard approximation tools (finite differences and finite elements) used in these works need to resolve all variations in the coefficients which ultimately leads to high-dimensional systems of linear equations and easily exceeds today's computational resources. Therefore, computational multiscale methods are required which deliver a macroscopic representation of the solution with drastically reduced computational effort. Prominent examples include the Heterogeneous

Multiscale Method (HMM) [EE03, EE05, AEEV12], the (Generalized) Multiscale Finite Element Method [HW97, EH09, EGH13], or the Localized Orthogonal Decomposition (LOD) [MP14, HP13].

The main contribution of this article are the presentation and numerical analysis of multiscale methods in the spirit of the LOD for the Helmholtz equation with Kerr-type nonlinearity. Various works have successfully applied the LOD to wave propagation problems such as the wave equation [AH17, MP19], the Helmholtz equation with constant [GP15, Pet17] and spatially varying coefficients [BGP17, PV20] as well as time-harmonic Maxwell's equations [GHV18, Ver17, HP20]. Besides dealing with multiscale coefficients, the LOD can also reduce the well-known pollution effect for the linear Helmholtz equation [GP15, Pet17]. However, those strategies for heterogeneous wave propagation problems mostly rely heavily on linear arguments. While the nonlinear Helmholtz equation is semi-linear, we cannot treat it as a small perturbation of a linear diffusion problem as in [HMP14a, HMP14b] because the wave number k may be very large and dominate the behavior of the solutions.

In this work, we combine ideas on (iterative) finite element approximations for the constant coefficient nonlinear Helmholtz equation [WZ18] and on the construction of multiscale spaces known from the LOD for nonlinear problems by linearization [Ver19]. More specifically, we present and analyze iterative multiscale approximations based on a fixed-point iteration for the nonlinear Helmholtz equation. We use an error indicator to locally decide in each step whether to update the multiscale basis. For sufficiently small tolerance employed in this decision, we show an a priori error estimate which is of optimal order in the mesh size – independent of the possible low regularity of the exact solution. We need to take into account this low regularity, i.e., not more than H^1, when estimating the non-linearity. Since our analysis is largely based on fixed-point arguments, the above results hold under the assumption of sufficiently small data ε and f. We emphasize, however, that even under this assumption the nonlinearity can be dominating due to large wave numbers k.

The paper is organized as follows. In Section 2, we introduce our model problem and show the existence and uniqueness of solutions under minimal regularity assumptions. These results complement [WZ18] and may be of own interest. Our multiscale approaches are introduced and analyzed in Section 3. Finally, numerical experiments in Section 4 illustrate our theoretical findings. More technical proofs of the main results are collected in the Appendix.

Notation. Unless otherwise mentioned, all our functions are complex-valued and we use $\overline{v}$ to denote the complex conjugate of v. For any (sub)domain S, $(\cdot, \cdot)_S$ denotes the standard L^2-scalar product (without complex conjugation in the second argument). Further, we use the following norms $\| \cdot \|_{0,S} := \| \cdot \|_{L^2(S)}$ and $| \cdot |_{1,S} := \| \nabla \cdot \|_{0,S}$. As usual in the Helmholtz context, we also employ the following k-weighted norm $\| \cdot \|_{1,k,S}^2 := | \cdot |_{1,S}^2 + k^2 \| \cdot \|_{0,S}^2$ with associated scalar product $(\cdot, \cdot)_{1,k,S}$. We will omit the subdomain S in the notation of norms and scalar products if it equals the full computational domain D and no confusion can arise. Last, we use the notation $a \lesssim b$ to indicate that there exists a generic constant C such that $a \leq Cb$.

2. Helmholtz Equation with Kerr-Type Nonlinearity

2.1. **Model problem.** Let $D \subset \mathbb{R}^d$, $d \in \{2,3\}$ be a bounded convex domain with Lipschitz boundary $\Gamma = \partial D$ and outer normal ν. Further, denote with $D_\varepsilon \subset \overline{D}_\varepsilon \subset D$ the subdomain which corresponds to a (nonlinear) Kerr medium.

In this work, we are interested in approximating the solution u of the following nonlinear Helmholtz problem,

$$
\begin{aligned}
-\mathrm{div} A \nabla u - k^2 n (1 + \varepsilon \mathbb{1}_{D_\varepsilon} |u|^2) u &= f \quad \text{in } D, \\
\nabla u \cdot \nu + \mathbf{i} k u &= 0 \quad \text{on } \Gamma,
\end{aligned}
\tag{2.1}
$$

where k is the wave number, n the refractive index, and ε the Kerr coefficient. Further, A is the diffusion coefficient. Note that ε, A, and n may depend on the spatial variable $x \in D$ and possibly vary on a fine scale. For simplicity, we only consider scalar-valued material coefficients A, but the extension to matrix-valued coefficients is straightforward. Moreover, other types of boundary conditions could be studied as well. We make the following assumptions on the data throughout the whole article.

Assumption 2.1. Suppose that
- $f \in L^2(D)$,
- $k \geq k_0 > 0$,
- n, ε, $A \in L^\infty(D; \mathbb{R})$ with $0 < c_n \leq n \leq C_n < \infty$, $0 \leq \varepsilon \leq C_\varepsilon < \infty$, and $0 < c_A \leq A \leq C_A < \infty$ uniformly in x,
- $\mathrm{supp}(1 - A)$ and $\mathrm{supp}(1 - n)$ are compactly embedded in D.

Note that the last assumption ensures that $A = 1$ and $n = 1$ at the boundary Γ. Since solutions to (2.1) might not exist in the classical sense, we now consider the weak formulation of finding $u \in H^1(D)$ that solves

$$
\mathcal{B}(u,v) := (A \nabla u, \nabla \overline{v}) - (k^2 n (1 + \varepsilon \mathbb{1}_{D_\varepsilon} |u|^2) u, \overline{v}) + \mathbf{i}(ku, \overline{v})_\Gamma = (f, \overline{v})
\tag{2.2}
$$

for all $v \in H^1(D)$.

The rest of this section is devoted to the existence and uniqueness of solutions to (2.2), see Theorem 2.7. The main idea is to approximate the solution u by a fixed-point iteration, as already suggested in [WZ18]. Due to the varying coefficients A and n, however, some alterations have to be made. First, the well-posedness of the auxiliary linear problem, where the nonlinearity is *fixed* (see the next section for a precise definition), is not clear from standard Helmholtz arguments. Second, since we allow for general L^∞-coefficients A and n we cannot necessarily expect solutions to linear Helmholtz problems to be in $H^2(D)$. Hence, one of the central arguments in [WZ18], namely L^∞-estimates for solutions to linear Helmholtz problems and the embedding of $H^2(D)$ into $L^\infty(D)$ for $d \in \{2,3\}$ have to be replaced by arguments using only H^1-regularity.

2.2. **Auxiliary linear problem.** In view of linearization strategies that will be used to solve (2.2), we now introduce an auxiliary linearized version of (2.2) which is characterized by $\mathcal{B}_{\mathrm{lin}}$ defined by

$$
\mathcal{B}_{\mathrm{lin}}(\Phi; u, v) := (A \nabla u, \nabla \overline{v}) - (k^2 n\, u, \overline{v}) - (k^2 n\, \varepsilon \mathbb{1}_{D_\varepsilon} |\Phi|^2 u, \overline{v}) + \mathbf{i}(ku, \overline{v})_\Gamma
\tag{2.3}
$$

for u, v, $\Phi \in H^1(D)$. The operator $\mathcal{B}_{\mathrm{lin}}$ is sesquilinear with respect to the last two arguments. The auxiliary linear problem then reads: given $\Phi \in H^1(D)$, find u_Φ that solves

$$
\mathcal{B}_{\mathrm{lin}}(\Phi; u_\Phi, v) = (f, \overline{v})
\tag{2.4}
$$

for all $v \in H^1(D)$. Note that $\mathcal{B}_{\mathrm{lin}}$ is bounded with respect to the second and third argument in the norm $\| \cdot \|_{1,k}$ provided that $k^2 n \, \varepsilon \mathbb{1}_{D_\varepsilon} |\Phi|^2$ can be bounded, see Proposition 2.4.

By setting $\Phi \equiv 0$, we obtain the *classical (linear) Helmholtz problem* that consists in finding $u_0 \in H^1(D)$ such that

$$(2.5) \qquad \mathcal{B}_{\mathrm{lin}}(0; u_0, v) = (f, \overline{v})$$

for all $v \in H^1(D)$. If the unique continuation principle holds, *Fredholm's alternative* can be employed to show that (2.5) possesses a unique solution. As discussed in [GPS19, GS20] in detail, Assumption 2.1 is sufficient for the unique continuation principle to hold for $d = 2$, whereas for $d = 3$ one has to make additional assumptions, e.g., $A \in C^{0,1}(D)$. Well-posedness of (2.5) via Fredholm's alternative, however, does not provide a quantitative stability estimate, in particular with a wave number explicit stability constant, for the solution u_0 of (2.5). Here, we base our analysis on the following assumption.

Assumption 2.2 (Well-posedness and stability of the classical Helmholtz problem). We assume that (2.5) possesses a unique solution and that there exists a constant $C_{\mathrm{stab},0}(k) > 0$ such that the solution $u_0 \in H^1(D)$ of (2.5) fulfills the stability estimate

$$(2.6) \qquad \|u_0\|_{1,k} \leq C_{\mathrm{stab},0}(k) \, \|f\|_0.$$

Note that several works consider the dependence of $C_{\mathrm{stab},0}(k)$ on the wave number k, also in the present setup of heterogeneous coefficients A and n, see, e.g., [BGP17, GPS19, MS19, ST18] and the references therein. For instance, [GPS19] proves that $C_{\mathrm{stab},0}(k) \lesssim 1$ under certain conditions on the Lipschitz coefficients A and n. The crucial point is to exclude the existence of so-called trapped rays in the setup, see the discussion and references in [GPS19, LSW20].

As a next step, we quantify the well-posedness of the auxiliary linear problem (2.4) based on the well-posedness of the classical Helmholtz problem. Therefore, we require a *Nirenberg-type inequality* which is stated in the following lemma.

Lemma 2.3 (Nirenberg-type inequality). There exists a constant $C_{\mathrm{Nir}} > 0$ such that

$$k^{1-d/3} \|v\|_{L^6(S)} \leq C_{\mathrm{Nir}} \|v\|_{1,k,S}.$$

for all $v \in H^1(D)$ and $S \subset D$.

Proof. From [Nir59], there exists a constant $C_{\mathrm{Nir}} > 0$ such that

$$\|v\|_{L^6(S)} \leq C_{\mathrm{Nir}} \, |v|_{1,S}^{d/3} \, \|v\|_{0,S}^{1-d/3}$$

for all $v \in H^1(S)$, $S \subset D$. Since $|v|_{1,S} \leq \|v\|_{1,k,S}$ and $k \|v\|_{0,S} \leq \|v\|_{1,k,S}$, we obtain

$$k^{1-d/3} \|v\|_{L^6(S)} \leq C_{\mathrm{Nir}} \, |v|_{1,S}^{d/3} \, k^{1-d/3} \|v\|_{0,S}^{1-d/3} \leq C_{\mathrm{Nir}} \|v\|_{1,k,S}. \qquad \square$$

Proposition 2.4. *Let* $\Phi \in H^1(D)$ *such that*

$$(2.7) \qquad C_{\mathrm{stab},0}(k) C_n C_\varepsilon C_{\mathrm{Nir}}^3 k^{d-1} \|\Phi\|_{1,k,D_\varepsilon}^2 \leq \vartheta < 1.$$

Then, there exists a unique solution u_Φ *of* (2.4) *and the stability estimate*

$$(2.8) \qquad \|u_\Phi\|_{1,k} \leq C_{\mathrm{stab}}(k) \, \|f\|_0$$

holds with $C_{\mathrm{stab}}(k) = (1 - \vartheta)^{-1} C_{\mathrm{stab},0}(k)$.

Further, the continuity constant of $\mathcal{B}_{\mathrm{lin}}$ *is given by* $C_{\mathcal{B}} = 2 \max\{C_A, C_n\} + (1 + 2 \, C_{\mathrm{tr}})$, *where* C_{tr} *denotes the constant in the trace inequality* (2.9).

Proof. Let $\Phi \in H^1(D)$. We define the operator $T: H^1(D) \to H^1(D)$, which maps $\psi \in H^1(D)$ to the solution $T\psi \in H^1(D)$ of the following Helmholtz problem

$$\mathcal{B}_{\text{lin}}(0; T\psi, v) = (f + k^2 n\varepsilon \mathbb{1}_{D_\varepsilon}|\Phi|^2\psi, \overline{v}).$$

The solution of the auxiliary linear problem (2.4) can then equivalently be formulated as the fixed-point problem $u_\Phi = Tu_\Phi$. The existence and uniqueness of the solution u_Φ of the auxiliary linear problem therefore follow from *Banach's fixed-point theorem* provided that T is a contraction.

To show the contraction property, let $\psi_1, \psi_2 \in H^1(D)$. We set $w := T\psi_1 - T\psi_2$ and observe that w solves

$$\mathcal{B}_{\text{lin}}(0; w, v) = (k^2 n\varepsilon \mathbb{1}_{D_\varepsilon}|\Phi|^2(\psi_1 - \psi_2), \overline{v})$$

for all $v \in H^1(D)$. With (2.6) and Lemma 2.3, we deduce

$$\begin{aligned}
\|T\psi_1 - T\psi_2\|_{1,k} &\leq C_{\text{stab},0}(k)\|k^2 n\varepsilon \mathbb{1}_{D_\varepsilon}|\Phi|^2(\psi_1 - \psi_2)\|_0 \\
&\leq C_{\text{stab},0}(k)k^2 C_n C_\varepsilon \|\Phi\|_{L^6(D_\varepsilon)}^2 \|\psi_1 - \psi_2\|_{L^6(D)} \\
&\leq C_{\text{stab},0}(k)C_n C_\varepsilon C_{\text{Nir}}^3 k^{d-1}\|\Phi\|_{1,k,D_\varepsilon}^2 \|\psi_1 - \psi_2\|_{1,k}.
\end{aligned}$$

The assumption (2.7) yields the desired contraction and the formula for $C_{\text{stab}}(k)$ immediately follows by means of a geometric series.

Regarding the continuity constant $C_\mathcal{B}$, we use the following *trace inequality* (see, e.g., [Gri85, Sec. 1.5]),

$$(2.9) \qquad \|u\|_{0,\Gamma}^2 \leq C_{\text{tr}}\|u\|_0\|u\|_1.$$

From this and using a weighted Young's inequality, we obtain

$$(2.10) \qquad \begin{aligned}
|\mathbf{i}(ku, v)| &\leq C_{\text{tr}}k\|u\|_0^{1/2}\|u\|_1^{1/2}\|v\|_0^{1/2}\|v\|_1^{1/2} \\
&\leq C_{\text{tr}}(k\|u\|_0 + \|u\|_1)(k\|v\|_0 + \|v\|_1) \\
&\leq 2\,C_{\text{tr}}\|u\|_{1,k}\|v\|_{1,k}.
\end{aligned}$$

With Lemma 2.3 and (2.7), we further have the rough estimate

$$(2.11) \qquad |(k^2 n\,\varepsilon \mathbb{1}_{D_\varepsilon}|\Phi|^2 u, \overline{v})| \leq k^2 C_n C_\varepsilon \|\Phi\|_{L^6(D_\varepsilon)}^2 \|u\|_{L^6(D)}\|v\|_0 \leq \vartheta\|u\|_{1,k}\|v\|_{1,k}.$$

With (2.10) and (2.11), we finally compute

$$\begin{aligned}
|\mathcal{B}_{\text{lin}}(\Phi; u, v)| &= |(A\nabla u, \nabla \overline{v}) - (k^2 n\,u, \overline{v}) - (k^2 n\,\varepsilon \mathbb{1}_{D_\varepsilon}|\Phi|^2 u, \overline{v}) + \mathbf{i}(ku, \overline{v})_\Gamma| \\
&\leq C_A|u|_1|v|_1 + C_n k^2\|u\|_0\|v\|_0 + (\vartheta + 2C_{\text{tr}})\|u\|_{1,k}\|v\|_{1,k} \\
&\leq \big(2\max\{C_A, C_n\} + (1 + 2\,C_{\text{tr}})\big)\|u\|_{1,k}\|v\|_{1,k}. \qquad \square
\end{aligned}$$

Remark 2.5. With the same techniques, one can as well show the existence and uniqueness of the solution to the adjoint problem.

2.3. **Existence and stability of solutions to the nonlinear problem.** Based on the iterative procedure used in [WZ18], we now show existence and stability results for the nonlinear problem (2.2) based on the auxiliary problem (2.4) and the stability property quantified in Proposition 2.4.

Let $u^0 \in H^1(D)$. Employing the linearized Helmholtz problem (2.4), we consider the sequence of solutions $u^m \in H^1(D)$, $m \in \mathbb{N}$, which solve the sequence of problems given by

$$(2.12) \qquad \mathcal{B}_{\text{lin}}(u^{m-1}; u^m, v) = (f, \overline{v}).$$

As a first step, we show that if condition (2.7) holds for $\Phi = u^0$, it also holds for u^m, $m \in \mathbb{N}$, such that the stability estimate (2.8) is valid for the whole sequence $\{u^m\}_{m \in \mathbb{N}}$.

Lemma 2.6 (Stability of iterative solutions). *Let $u^0 \in H^1(D)$ such that (2.7) is fulfilled for $\Phi = u^0$. Further, suppose that*

$$(2.13) \qquad C_{\mathrm{stab},0}(k)C_{\mathrm{stab}}^2(k)C_n C_\varepsilon C_{\mathrm{Nir}}^3 \, k^{d-1} \, \|f\|_0^2 \leq \vartheta.$$

Then, the sequence $\{u^m\}_{m \in \mathbb{N}}$ defined by (2.12) fulfills the stability property

$$(2.14) \qquad \|u^m\|_{1,k} \leq C_{\mathrm{stab}}(k) \, \|f\|_0$$

for all $m \in \mathbb{N}$ with the constant $C_{\mathrm{stab}}(k)$ from Proposition 2.4.

Note that $C_{\mathrm{stab}}(k) = (1-\vartheta)^{-1}C_{\mathrm{stab},0}(k)$ in Proposition 2.4 so that in fact (2.13) is equivalent ot the following condition

$$C_{\mathrm{stab},0}(k)^3 C_n C_\varepsilon C_{\mathrm{Nir}}^3 \, k^{d-1} \, \|f\|_0^2 \leq \vartheta(1-\vartheta)^2.$$

Proof of Lemma 2.6. With (2.13) and (2.14) for some fixed $m \in \mathbb{N}$, we have that

$$C_{\mathrm{stab},0}(k)C_n C_\varepsilon C_{\mathrm{Nir}}^3 \, k^{d-1} \, \|u^{m+1}\|_{1,k,D_\varepsilon}^2 \leq C_{\mathrm{stab},0}(k)C_{\mathrm{stab}}^2(k)C_n C_\varepsilon C_{\mathrm{Nir}}^3 \, k^{d-1} \, \|f\|_0^2 \leq \vartheta.$$

The assertion thus follows by induction using Proposition 2.4. $\qquad\qquad \square$

As a next step, we use the sequence $\{u^m\}_{m \in \mathbb{N}}$ to show existence and uniqueness of the solution $u \in H^1(D)$ of (2.2).

Theorem 2.7 (Well-posedness of the nonlinear Helmholtz problem). *Let $u^0 \in H^1(D)$ such that (2.7) is fulfilled for $\Phi = u^0$. Further, suppose the following slightly stronger version of (2.13) holds,*

$$(2.15) \qquad 2 \, C_{\mathrm{stab}}^3(k)C_n C_\varepsilon C_{\mathrm{Nir}}^3 \, k^{d-1} \, \|f\|_0^2 \leq \vartheta.$$

Then, there exists a unique solution $u \in H^1(D)$ of (2.2) that fulfills the stability estimate

$$(2.16) \qquad \|u\|_{1,k} \leq C_{\mathrm{stab}}(k) \, \|f\|_0.$$

Before we prove the Theorem, some remarks on the assumptions are in order. We can again use $C_{\mathrm{stab}}(k) = (1-\vartheta)^{-1}C_{\mathrm{stab},0}(k)$ to equivalently write (2.15) in the following form

$$2 \, C_{\mathrm{stab},0}^3(k)C_n C_\varepsilon C_{\mathrm{Nir}}^3 \, k^{d-1} \, \|f\|_0^2 \leq \vartheta(1-\vartheta)^3.$$

Note that if we choose $u^0 = 0$, condition (2.7) is automatically satisfied for any choice of $0 < \vartheta < 1$ so that we basically require

$$2 \, C_{\mathrm{stab},0}^3(k)C_n C_\varepsilon C_{\mathrm{Nir}}^3 \, k^{d-1} \, \|f\|_0^2 < 1$$

in Theorem 2.7. This is sometimes termed as *smallness of the data assumption* because it requires the combination of wave number, refractive index, Kerr coefficient, volume, and boundary sources to be sufficiently small. The structure of this condition is of course very similar to [WZ18] and the main difference is that we have a factor k^{d-1} instead of the (better) factor k^{d-2} in [WZ18]. This, however, is to be expected since we estimate everything in H^1-norms whereas [WZ18] also employs H^2-norms.

Proof of Theorem 2.7. The proof follows the ideas of [WZ18, Thm. 2.5]. Let $\{u^m\}_{m\in\mathbb{N}}$ be the sequence of solutions defined in (2.12). We set $w^m := u^{m+1} - u^m$ and observe that w^m solves

$$\mathcal{B}_{\mathrm{lin}}(u^m; w^m, v) = (k^2 n\varepsilon\mathbb{1}_{D_\varepsilon}(|u^m|^2 - |u^{m-1}|^2)u^m, \overline{v})$$

for all $v \in H^1(D)$. Since (2.15) implies (2.13), we obtain with Lemma 2.6 and Lemma 2.3

$$\begin{aligned}
\|w^m\|_{1,k} &\leq C_{\mathrm{stab}}(k) \left\| k^2 n\varepsilon(|u^m|^2 - |u^{m-1}|^2)u^m \right\|_{0,D_\varepsilon} \\
&\leq C_{\mathrm{stab}}(k)\, k^2 C_n C_\varepsilon \|u^m\|_{L^6(D_\varepsilon)} \left(\|u^m\|_{L^6(D_\varepsilon)} + \|u^{m-1}\|_{L^6(D_\varepsilon)} \right) \|w^{m-1}\|_{L^6(D_\varepsilon)} \\
&\leq 2\, C_{\mathrm{stab}}^3(k) C_n C_\varepsilon C_{\mathrm{Nir}}^3\, k^{d-1} \|f\|_0^2 \|w^{m-1}\|_{1,k} \\
&\leq \vartheta\|w^{m-1}\|_{1,k}.
\end{aligned}$$

Therefore, $\{u^m\}_{m\in\mathbb{N}}$ is a Cauchy sequence with respect to $\|\cdot\|_{1,k}$ and converges to a limit $u := \lim_{m\to\infty} u^m \in H^1(D)$ which solves (2.2). The stability estimate (2.16) directly follows from (2.14).

To show uniqueness, let u and $\hat{u}$ be two solutions of (2.2). Then, $w := u - \hat{u}$ solves

$$\mathcal{B}_{\mathrm{lin}}(u; w, v) = (k^2 n\varepsilon\mathbb{1}_{D_\varepsilon}(|u|^2 - |\hat{u}|^2)\hat{u}, \overline{v})$$

for all $v \in H^1(D)$. As above, we thus get

$$(2.17) \qquad\qquad \|w\|_{1,k} \leq \vartheta\|w\|_{1,k},$$

which implies $w = 0$ because of $\vartheta < 1$. □

Remark 2.8. Since we do not exploit any higher regularity of solutions, the procedure in this section can verbatim be used to show existence and uniqueness of discrete solutions. More precisely, let $V \subset H^1(D)$ be a closed subspace and further, let Assumption 2.2 be satisfied in V and assume that (2.15) holds accordingly. With an appropriate initial iterate $v^0 \in V$ (e.g., $v^0 = 0$) and the arguments in Proposition 2.4, we directly obtain the existence and uniqueness of a Galerkin solution $v \in V$ to the Kerr-Helmholtz problem (2.2). Note, however, that the stability constants $C_{\mathrm{stab},0}(k)$ and thus $C_{\mathrm{stab}}(k)$ may generally depend on the subspace V.

3. Multiscale Approximations

In this section, we are concerned with the approximation of the solution of (2.2) in a finite-dimensional subspace. Since the present setting involves possible fine oscillations in the coefficients A, n, and ε, a classical finite element approximation requires a resolution of any fine-scale features in order to provide reasonable approximations; see, e.g., [BGP17, PV20] in the context of the linear Helmholtz problem. Additionally, discretizations of the Helmholtz problem are subject to the so-called *pollution effect* (see [BS97] and the references therein), so that for the lowest order finite element method the condition $kh^2 \lesssim 1$ typically has to be satisfied before convergence of the error is observed; see, e.g., [BGT85, AKS88]. Especially in the nonlinear setting where an iterative scheme is to be used, the required resolution of fine-scale features and the pollution effect lead to unfeasibly expensive computations.

The multiscale construction that is presented in this section aims at resolving this issue by constructing appropriate approximation spaces on a coarse-scale level. The approach is based on the Localized Orthogonal Decomposition method, which was introduced in [MP14] and further developed in [HP13] for an elliptic model problem. The coarse-scale

level is characterized by the mesh size H of a shape regular and quasi uniform quadri-lateral mesh $\mathcal{T}_H$. This mesh is coarse in the sense that it does not resolve the fine-scale features of the coefficients A, n, and ε. Denote by $Q_1(\mathcal{T}_H)$ the space of possibly discontinuous functions that are polynomials of coordinate degree at most one on each element of $\mathcal{T}_H$. We set $V_H := Q_1(\mathcal{T}_H) \cap H^1(D)$ the coarse Lagrange finite element space. The LOD approach is based upon a so-called quasi-interpolation operator $\mathcal{I}_H \colon H^1(D) \to V_H$ with the following properties

$$(3.1) \qquad H^{-1} \|(1 - \mathcal{I}_H)v\|_{0,T} + |\mathcal{I}_H v|_{1,T} \le \tilde{C}_{\mathrm{int}} |v|_{1,\mathrm{N}(T)}, \quad v \in H^1(D),$$

$$(3.2) \qquad \|\mathcal{I}_H v\|_{0,T} \le \tilde{C}_{\mathrm{int}} \|v\|_{0,\mathrm{N}(T)}, \quad v \in L^2(D),$$

$$(3.3) \qquad \mathcal{I}_H \circ \mathcal{I}_H = \mathcal{I}_H,$$

where $\mathrm{N}(T)$ denotes the neighborhood of the element $T \in \mathcal{T}_H$ defined by

$$\mathrm{N}(T) := \bigcup \{K \in \mathcal{T}_H : \overline{K} \cap \overline{T} \neq \emptyset\}.$$

The particular choice that we use in our numerical experiments is $\mathcal{I}_H := \pi_H \circ \Pi_H$, where Π_H is the piecewise L^2-projection onto $Q_1(\mathcal{T}_H)$. Moreover, π_H denotes an averaging operator that, for any $v_H \in Q_1(\mathcal{T}_H)$ and any vertex z of $\mathcal{T}_H$, is characterized by

$$\big(\pi_H(v_H)\big)(z) := \sum_{\substack{K \in \mathcal{T}_H: \\ z \in K}} \big(v_H|_K\big)(z) \cdot \frac{1}{\mathrm{card}\{T \in \mathcal{T}_H : z \in T\}}.$$

This choice of $\mathcal{I}_H$ satisfies the properties (3.1)–(3.3). We refer to [Osw93, Bre94, EG17] for a proof of these conditions. Note that from (3.1)–(3.2), we can directly derive the following estimates on the whole domain D,

$$(3.4) \qquad H^{-1} \|(1 - \mathcal{I}_H)v\|_0 + |\mathcal{I}_H v|_1 \le C_{\mathrm{int}} |v|_1, \quad v \in H^1(D),$$

$$(3.5) \qquad \|\mathcal{I}_H v\|_0 \le C_{\mathrm{int}} \|v\|_0, \quad v \in L^2(D).$$

Based on the operator $\mathcal{I}_H$, we define the so-called *fine-scale space* $\mathcal{W}$ as its kernel with respect to H^1-functions, i.e.,

$$\mathcal{W} := \ker \mathcal{I}_H|_{H^1(D)}.$$

Next, we define an auxiliary corrector problem based on a function Φ that fulfills (2.7) as follows. Let $\Phi \in H^1(D)$ be given and define the *correction operator* $\mathcal{C}_\Phi \colon H^1(D) \to \mathcal{W}$ for any $v \in H^1(D)$ as the solution of

$$(3.6) \qquad \mathcal{B}_{\mathrm{lin}}(\Phi; \mathcal{C}_\Phi v, w) = \mathcal{B}_{\mathrm{lin}}(\Phi; v, w)$$

for all $w \in \mathcal{W}$. Similarly, we also define the *adjoint correction operator* $\mathcal{C}_\Phi^* \colon H^1(D) \to \mathcal{W}$ for any $v \in H^1(D)$ as the solution of

$$(3.7) \qquad \mathcal{B}_{\mathrm{lin}}(\Phi; w, \mathcal{C}_\Phi^* v) = \mathcal{B}_{\mathrm{lin}}(\Phi; w, v)$$

for all $w \in \mathcal{W}$ and remark that $\mathcal{C}_\Phi^* v = \overline{\mathcal{C}_\Phi \overline{v}}$.

Note that (3.6) and (3.7) are well-defined by the coercivity condition that is proved in the following lemma.

Lemma 3.1 (coercivity condition on $\mathcal{W}$). Let $\Phi \in H^1(D)$ fulfill (2.7). Assume that

$$(3.8) \qquad kH \le C_{\mathrm{res}} := \frac{\sqrt{c_A}}{2 C_{\mathrm{int}} \sqrt{C_n}}$$

and

$$(3.9) \qquad 2\, C_{\text{int}}^{2-d/3} C_{\text{res}}^{1-d/3} \vartheta H \leq C_{\text{stab},0}(k)\, c_A.$$

Then, it holds that

$$(3.10) \qquad \Re \mathcal{B}_{\text{lin}}(\Phi; w, w) \geq \gamma \|w\|_{1,k}^2$$

for all $w \in \mathcal{W}$ with $\gamma := \frac{c_A C_n}{4C_n + c_A}$.

Let us comment on the assumptions of Lemma 3.1. First, (3.8) requires kH to be sufficiently small (of the order one), which is a natural resolution condition because one always needs some degrees of freedom per wave length to faithfully represent the wave. Second, we emphasize that (3.9) does *not* result in a (notable) restriction of the mesh size in particular for growing wave numbers: the left-hand side factors $C_{\text{int}}^{2-d/3} C_{\text{res}}^{1-d/3} \vartheta$ are independent of k and of order one. On the right-hand side, $C_{\text{stab},0}(k)$ in most cases is of order k^q with some $q \geq 0$ so that it remains constant or is even growing with increasing k. Hence, (3.9) is no resolution condition that requires H to become smaller for large frequencies. In fact, (3.8) will in practice, especially for large k, be the dominating and important condition. Finally, we mention that the dependency of (3.8) and (3.9) on c_A may be removed by the use of A-weighted norms and suitable A-weighted interpolation operators, which is relevant in the high contrast case, where c_A might be very small. This, however, is not the focus of the present work and we refer to [PV20], for instance, for details in the context of the linear Helmholtz problem.

Proof of Lemma 3.1. By the definition of $\mathcal{W} = \ker \mathcal{I}_H|_{H^1(D)}$ and (3.4), we have for any $w \in \mathcal{W}$

$$(3.11) \qquad \|w\|_0 = \|(1 - \mathcal{I}_H)w\|_0 \leq C_{\text{int}} H \, |w|_1.$$

From (3.11) and (3.8), we also get that $|\cdot|_1$ is a norm on $\mathcal{W}$ which is equivalent to the full norm $\|\cdot\|_1$ as well as the energy norm $\|\cdot\|_{1,k}$ with constants that are independent of k and H. In particular, for any $w \in \mathcal{W}$,

$$(3.12) \qquad |w|_1 \leq \|w\|_1 \leq (1 + C_{\text{int}}^2 H^2)^{1/2} |w|_1 \leq (1 + C_{\text{int}}^2)^{1/2} |w|_1$$

and

$$(3.13) \qquad |w|_1 \leq \|w\|_{1,k} \leq (1 + C_{\text{int}}^2 C_{\text{res}}^2)^{1/2} |w|_1.$$

Further, using Lemma 2.3, (3.11), and (2.7), we have that

$$
\begin{aligned}
(3.14) \quad k^2 C_n C_\varepsilon \|\Phi\|_{L^6(D_\varepsilon)}^2 & \|w\|_{L^6(D)} \|w\|_0 \\
&\leq C_n C_\varepsilon C_{\text{Nir}}^2 C_{\text{int}} H k^{2d/3} \|\Phi\|_{1,k,D_\varepsilon}^2 \|w\|_{L^6(D)} |w|_1 \\
&\leq C_n C_\varepsilon C_{\text{Nir}}^3 C_{\text{int}} H k^{d-1} \|\Phi\|_{1,k,D_\varepsilon}^2 |w|_1^{d/3} k^{1-d/3} \|w\|_0^{1-d/3} |w|_1 \\
&\leq C_n C_\varepsilon C_{\text{Nir}}^3 C_{\text{int}}^{2-d/3} H (k^{1-d/3} H^{1-d/3}) k^{d-1} \|\Phi\|_{1,k,D_\varepsilon}^2 |w|_1^2 \\
&\leq C_{\text{int}}^{2-d/3} C_{\text{res}}^{1-d/3} (C_{\text{stab},0}(k))^{-1} \vartheta H |w|_1^2 \leq \frac{c_a}{2} |w|_1^2,
\end{aligned}
$$

where we applied assumption (3.9) in the last step. Therefore, with (3.12), (3.14), and the inclusion $H^1(D) \subset L^6(D)$, we obtain for any $w \in \mathcal{W}$

$$
\begin{aligned}
\Re \mathcal{B}_{\mathrm{lin}}(\Phi; w, w) \geq \Re \mathcal{B}_{\mathrm{lin}}(\Phi; w, w) &= (A \nabla w, \nabla \overline{w}) - (k^2 n (1 + \varepsilon |\Phi|^2) w, \overline{w}) \\
&\geq c_A |w|_1^2 - C_{\mathrm{int}}^2 C_{\mathrm{res}}^2 C_n |w|_1^2 - \tfrac{c_A}{2} |w|_1^2 \\
&= \left(\frac{c_A}{2} - C_{\mathrm{int}}^2 C_{\mathrm{res}}^2 C_n \right) |w|_1^2.
\end{aligned}
$$

The assertion follows with the definitions of C_{res} and γ. $\qquad \square$

3.1. **Stability and error estimates for the auxiliary multiscale solution.** Based on $\Phi \in H^1(D)$ as above, we define the multiscale solution corresponding to (2.4) as the solution $u_{\Phi,H} \in (1 - \mathcal{C}_\Phi) V_H$ of

$$
(3.15) \qquad \qquad \mathcal{B}_{\mathrm{lin}}(\Phi; u_{\Phi,H}, v_H) = (f, \overline{v_H})
$$

for all $v_H \in (1 - \mathcal{C}_\Phi^*) V_H$. If the above assumptions on Φ are satisfied, we can deduce that $\mathcal{B}_{\mathrm{lin}}(\Phi; \cdot, \cdot)$ fulfills an inf-sup-condition on $H^1(D)$ as quantified in the next lemma.

Lemma 3.2 (Inf-sup-condition on $H^1(D)$). Assume that (2.7) is satisfied. Then, we have that

$$
(3.16) \qquad \qquad \inf_{v \in H^1(D)} \sup_{w \in H^1(D)} \frac{\Re \mathcal{B}_{\mathrm{lin}}(\Phi; v, w)}{\|v\|_{1,k} \|w\|_{1,k}} \geq \delta(k)
$$

with $\delta(k) = \frac{\min\{c_A, c_n\}}{C_{\mathrm{stab}}(k)(2\,k C_n + 1)}$.

Proof. The proof follows the ideas of [Pet17, Lemma 2.1]. Let $v \in H^1(D)$ be given and define $z \in H^1(D)$ as the solution of

$$
\mathcal{B}_{\mathrm{lin}}(\Phi; w, z) = (k^2 n (2 + \varepsilon \mathbb{1}_{D_\varepsilon} |\Phi|^2) v, \overline{w})
$$

for all $w \in H^1(D)$. From Proposition 2.4, Remark 2.5, and Lemma 2.3, we know that z exists, is unique and satisfies

$$
\begin{aligned}
\|z\|_{1,k} &\leq C_{\mathrm{stab}}(k) \big(2\, C_n k^2 \|v\|_0 + C_n C_\varepsilon C_{\mathrm{Nir}}^3 k^{d-1} \|\Phi\|_{1,k,D_\varepsilon}^2 \|v\|_{1,k} \big) \\
&\leq C_{\mathrm{stab}}(k)(2\, k C_n + 1) \|v\|_{1,k}.
\end{aligned}
$$

We set $w = v + z$. The assertion then follows from the inequality

$$
\Re \mathcal{B}_{\mathrm{lin}}(\Phi; v, w) \geq \min\{c_A, c_n\} \|v\|_{1,k}^2. \qquad \square
$$

Based on Lemma 3.1 and Lemma 3.2, it is possible to show stability and error estimates for the solution $u_{\Phi,H}$ of (3.15) as stated in the following lemma.

Lemma 3.3 (Stability and approximation properties of the auxiliary multiscale solution). Let $u_\Phi \in H^1(D)$ be the solution of (2.4) and $u_{\Phi,H} \in H^1(D)$ the solution of (3.15). If the assumptions of Lemma 3.1 hold, we have that

$$
(3.17) \qquad \qquad \|u_{\Phi,H}\|_{1,k} \leq C_{\mathrm{LOD}}(k) \|f\|_0.
$$

with $C_{\mathrm{LOD}}(k) := \frac{C_{\mathcal{B}}}{\delta(k)\gamma}$ with $C_{\mathcal{B}}$ from Proposition 2.4, $\delta(k)$ from Lemma 3.2, and γ from Lemma 3.1. Further,

$$
(3.18) \qquad \qquad \|u_\Phi - u_{\Phi,H}\|_{1,k} \leq C_{\mathrm{err}} H \|f\|_0,
$$

where $C_{\mathrm{err}} := \gamma^{-1} C_{\mathrm{int}}$.

Proof. The proof is similar as for linear Helmholtz problems in [Pet17, PV20] and we present it here for convenience and to make the material self-consistent.

Proof of (3.17): We prove the following inf-sup-condition

$$\inf_{v_H \in V_H} \sup_{w_H \in V_H} \frac{\Re \mathcal{B}_{\mathrm{lin}}(\Phi; (1 - \mathcal{C}_\Phi)v_H, (1 - \mathcal{C}_\Phi^*)w_H)}{\|(1 - \mathcal{C}_\Phi)v_H\|_{1,k} \|(1 - \mathcal{C}_\Phi^*)w_H\|_{1,k}} \geq \frac{\delta(k)\gamma}{C_\mathcal{B}},$$

which directly implies (3.17). To show the inf-sup-condition, let $v_H \in V_H$ be arbitrary but fixed. Due to (3.16), there exists $w \in H^1(D)$ with $\|w\|_{1,k} = 1$ such that

$$\Re \mathcal{B}_{\mathrm{lin}}(\Phi; (1 - \mathcal{C}_\Phi)v_H, w) \geq \delta(k)\|(1 - \mathcal{C}_\Phi)v_H\|_{1,k}.$$

We set $w_H = \mathcal{I}_H w$ and observe that $(1 - \mathcal{C}_\Phi^*)w_H = (1 - \mathcal{C}_\Phi^*)w$. Therefore, with (3.16) and the continuity of $\mathcal{B}_{\mathrm{lin}}$, we deduce that

$$\Re \mathcal{B}_{\mathrm{lin}}(\Phi; (1 - \mathcal{C}_\Phi)v_H, (1 - \mathcal{C}_\Phi^*)w_H) = \Re \mathcal{B}_{\mathrm{lin}}(\Phi; (1 - \mathcal{C}_\Phi)v_H, w) \geq \delta(k)\|(1 - \mathcal{C}_\Phi)v_H\|_{1,k}.$$

The inf-sup-condition follows by the norm equivalence

$$\|(1 - \mathcal{C}_\Phi^*)w_H\|_{1,k} \leq C_\mathcal{B}\gamma^{-1}\|w\|_{1,k}$$

due to the stability of the corrector problems, see, e.g., [Pet17] for details.

Proof of (3.18): A simple calculation shows that $u_{\Phi,H} = (1 - \mathcal{C}_\Phi)\mathcal{I}_H u_\Phi = (1 - \mathcal{C}_\Phi)u$ and hence, $u - u_{\Phi,H} = \mathcal{C}_\Phi u \in \mathcal{W}$. By the definition of $\mathcal{C}_\Phi$ in (3.6), the error $u - u_{\Phi,H}$ therefore satisfies

$$\mathcal{B}_{\mathrm{lin}}(\Phi; \mathcal{C}_\Phi u, \mathcal{C}_\Phi u) = \mathcal{B}_{\mathrm{lin}}(\Phi; u, \mathcal{C}_\Phi u) = (f, \overline{\mathcal{C}_\Phi u}).$$

Lemma 3.1 and (3.4) then yield

$$\|u - u_{\Phi,H}\|_{1,k}^2 \leq \gamma^{-1}(f, \overline{\mathcal{C}_\Phi u}) \leq \gamma^{-1}C_{\mathrm{int}}H\|f\|_0\|u - u_{\Phi,H}\|_{1,k},$$

which finishes the proof. $\qquad\qquad\square$

3.2. Iterative multiscale approximation.

In this subsection, we define a sequence of multiscale solutions $\{u_H^m\}_{m \in \mathbb{N}}$. To this end, we abbreviate $\mathcal{C}_m := \mathcal{C}_{u_H^m}$ and define $u_H^m \in (1 - \mathcal{C}_{m-1})V_H$ as the solution of

$$(3.19) \qquad\qquad \mathcal{B}_{\mathrm{lin}}(u_H^{m-1}; u_H^m, v_H) = (f, \overline{v_H})$$

for all $v_H \in (1 - \mathcal{C}_{m-1}^*)V_H$ and given $u_H^0 \in H^1(D)$ as, e.g., a first-order approximation of u^0,

$$(3.20) \qquad\qquad \|u_H^0 - u^0\|_{1,k} \leq C_0 H.$$

Note that the functions $\{u_H^m\}_{m \in \mathbb{N}}$ fulfill similar stability properties as in Lemma 2.6. However, the stability constant $C_{\mathrm{stab}}(k)$ needs to be replaced by $C_{\mathrm{LOD}}(k)$ from Lemma 3.3. Since $C_{\mathrm{LOD}}(k)$ is based on the inf-sup-condition, this in particular includes an additional factor of k.

Based on these observations, we prove in the following theorem that the solutions $\{u_H^m\}_{m \in \mathbb{N}}$ are close to the iterative solutions $\{u^m\}_{m \in \mathbb{N}}$ of (2.12) with respect to the mesh size H.

Theorem 3.4. *Define $\tilde{C}_{\mathrm{stab}}(k) := \max\{C_{\mathrm{stab}}(k), C_{\mathrm{LOD}}(k)\}$ with the constants $C_{\mathrm{stab}}(k)$ and $C_{\mathrm{LOD}}(k)$ from Proposition 2.4 and Lemma 3.3, respectively. Further, assume that*

$$(3.21) \qquad\qquad 2\,\tilde{C}_{\mathrm{stab}}^3(k)C_n C_\varepsilon C_{\mathrm{Nir}}^3\, k^{d-1}\, \|f\|_0^2 \leq \vartheta.$$

Then, we have that

$$(3.22) \qquad \|u_H^m - u^m\|_{1,k} \le \vartheta^m \|u_H^0 - u^0\|_{1,k} + \frac{1}{1-\vartheta} C_{\mathrm{err}} H \|f\|_0$$

for all $m \in \mathbb{N}$.

Proof. Let $m \in \mathbb{N}$ be fixed. We define an auxiliary solution $w^m \in H^1(D)$ as the solution of

$$(3.23) \qquad \mathcal{B}_{\mathrm{lin}}(u_H^{m-1}; w^m, v) = (f, \overline{v})$$

for all $v \in H^1(D)$. Note that due to (3.21) and by Proposition 2.4 (as well as its adapted version for the series of multiscale solutions), we have the following stability estimates,

$$(3.24) \qquad \|u_H^{m-1}\|_{1,k} \le C_{\mathrm{LOD}}(k) \|f\|_0,$$
$$(3.25) \qquad \|u^m\|_{1,k} \le C_{\mathrm{stab}}(k) \|f\|_0,$$
$$(3.26) \qquad \|w^m\|_{1,k} \le C_{\mathrm{stab}}(k) \|f\|_0.$$

Further, the error $e^m = u^m - w^m$ solves

$$\begin{aligned}
\mathcal{B}_{\mathrm{lin}}(u^{m-1}; e^m, v) &= \mathcal{B}_{\mathrm{lin}}(u_H^{m-1}; w^m, v) - \mathcal{B}_{\mathrm{lin}}(u^{m-1}; w^m, v) \\
&= (k^2 \varepsilon \mathbb{1}_{D_\varepsilon}(|u^{m-1}|^2 - |u_H^{m-1}|^2) w^m, \overline{v})
\end{aligned}$$

for all $v \in H^1(D)$. Reusing ideas from Theorem 2.7 and with the boundedness of w, u^{m-1}, and u_H^{m-1} as quantified in (3.24)–(3.26), we obtain

$$\begin{aligned}
\|e^m\|_{1,k} &\le C_{\mathrm{stab}}(k) \|k^2 \varepsilon \mathbb{1}_{D_\varepsilon}(|u^{m-1}|^2 - |u_H^{m-1}|^2) w^m\|_{0,D_\varepsilon} \\
&\le C_{\mathrm{stab}}(k) k^2 C_n C_\varepsilon \|w^m\|_{L^6(D_\varepsilon)} \\
&\qquad \cdot \left(\|u^{m-1}\|_{L^6(D_\varepsilon)} + \|u_H^{m-1}\|_{L^6(D_\varepsilon)} \right) \|u_H^{m-1} - u^{m-1}\|_{L^6(D_\varepsilon)} \\
&\le \vartheta \|u_H^{m-1} - u^{m-1}\|_{1,k}.
\end{aligned}$$

Moreover, with Lemma 3.3 we have that

$$\|u_H^m - w^m\|_{1,k} \le C_{\mathrm{err}} H \|f\|_0.$$

The previous two estimates and the triangle inequality result in

$$\begin{aligned}
\|u_H^m - u^m\|_{1,k} &\le \|e^m\|_{1,k} + \|u_H^m - w^m\|_{1,k} \\
&\le \vartheta \|u_H^{m-1} - u^{m-1}\|_{1,k} + C_{\mathrm{err}} H \|f\|_0 \\
&\le \vartheta^m \|u_H^0 - u^0\|_{1,k} + C_{\mathrm{err}} H \|f\|_0 \sum_{n \in \mathbb{N}_0} \vartheta^n \\
&\le \vartheta^m \|u_H^0 - u^0\|_{1,k} + \frac{1}{1-\vartheta} C_{\mathrm{err}} H \|f\|_0. \qquad \square
\end{aligned}$$

With Theorem 3.4, we can directly derive the following result.

Corollary 3.5. *Suppose that the assumptions of Theorem 3.4 are satisfied. Let u_H^m be the iterative multiscale approximation in step m starting from the initial value $u_H^0 = 0$. Then, it holds that*

$$\|u - u_H^m\|_{1,k} \le \frac{1}{1-\vartheta}(C_{\mathrm{stab},0}(k)\vartheta^m + C_{\mathrm{err}}H)\|f\|_0.$$

Proof. Approximate u by the fixed-point iteration starting from the initial value $u^0 = 0$. By the triangle inequality, we have $\|u - u_H^m\|_{1,k} \leq \|u - u^m\|_{1,k} + \|u^m - u_H^m\|_{1,k}$, where the latter term is estimated with Theorem 3.4. The a priori estimate for the fixed-point iteration together with (2.6) then yields

$$\|u - u^m\|_{1,k} \leq \frac{\vartheta^m}{1-\vartheta}\|u^1 - u^0\|_{1,k} \leq \frac{\vartheta^m}{1-\vartheta}C_{\text{stab},0}(k)\|f\|_0. \qquad \square$$

We emphasize that the multiscale procedure introduced in this section (cf. e.g. (3.15)) is *ideal* in the sense that for given $\Phi \in H^1(D)$, the correction operators $\mathcal{C}_\Phi$ and $\mathcal{C}_\Phi^*$ defined in (3.6) and (3.7), respectively, are global operations on the infinite-dimensional space $\mathcal{W}$. For practical computations, these operators are defined element-wise and truncated to local patches with ℓ layers of elements around each element. We will introduce and use this localization in the following subsection for our adaptive iterative multiscale approximation, which covers (3.19) as special case.

Remark 3.6. Note that in practical computations, the correction operators also need to be discretized on a fine mesh with mesh size $h \ll H$ that resolves possible oscillations. This is required in order to obtain a fully practical method. We omit this last step in the present work and refer to [GP15] for the corresponding analysis.

3.3. **Adaptive iterative multiscale approximation.** As mentioned, the goal of this subsection is two-fold. First, we localize the computation of the correction operators. Second, we introduce at the same time a strategy to (locally) decide where these correction operators need to be updated from one iteration step to the other. The motivation for this adaptive strategy is that updating the correction operators in each step is computationally rather expensive and might be unnecessary if the multiscale solutions only change in certain parts of the domain. Inspired by [HM19, HKM20], we will introduce an error indicator for the corrector if the function $\Phi \in H^1(D)$ is "perturbed". The numerical analysis of the resulting adaptive iterative multiscale algorithm is based on Theorem 3.4 from the previous section and the observation that the localization as well as the updating strategy both are small perturbations thereof.

We first introduce the localization of the correction operators. Recall the definition of $N(T)$ from Section 3. We inductively define the ℓ-layer patch for $\ell \in \mathbb{N}$ via

$$N^\ell(T) = N(N^{\ell-1}(T)), \quad \ell \geq 2, \quad \text{and} \quad N^1(T) = N(T).$$

The kernel space $\mathcal{W}$ is restricted to such element patches via

$$\mathcal{W}(N^\ell(T)) := \{w \in \mathcal{W} : w|_{D \setminus N^\ell(T)} = 0\}.$$

Given a function $\Phi \in H^1(D)$ and an element $T \in \mathcal{T}_H$, we define the ℓ-layer element corrector $\mathcal{C}_{\Phi,T}^\ell$ via the solution of a truncated and element-based corrector problem as follows. For any $v_H \in V_H$, we seek $\mathcal{C}_{\Phi,T}^\ell v_H \in \mathcal{W}(N^\ell(T))$ that solves

$$(3.27) \qquad \mathcal{B}_{\text{lin},N^\ell(T)}(\Phi; \mathcal{C}_{\Phi,T}^\ell v_H, w) = \mathcal{B}_{\text{lin},T}(\Phi; v_H, w)$$

for all $w \in \mathcal{W}(N^\ell(T))$. Here, $\mathcal{B}_{\text{lin},S}$ denotes the restriction of $\mathcal{B}_{\text{lin}}$ to the subdomain $S \subset D$. The globally defined ℓ-layer corrector $\mathcal{C}_\Phi^\ell$ is then given as the sum of the element correctors, i.e.,

$$\mathcal{C}_\Phi^\ell := \sum_{T \in \mathcal{T}_H} \mathcal{C}_{\Phi,T}^\ell.$$

The adjoint correction operator $\mathcal{C}_\Phi^{\ell,*}$ is defined analogously. If $\Phi \in H^1(D)$ satisfies (2.7) and the conditions (3.8)–(3.9) are fulfilled, the coercivity (3.10) from Lemma 3.1 implies that (3.27) is well-posed. Note that in order to compute $\mathcal{C}_{\Phi,T}^\ell$ it suffices to know Φ on $\mathrm{N}^\ell(T)$. The error between $\mathcal{C}_\Phi^\ell$ and $\mathcal{C}_\Phi$ is decaying exponentially in ℓ, which directly carries over from the linear case [GP15, BGP17].

Lemma 3.7. Let $\Phi \in H^1(D)$ satisfy (2.7). There exist $0 < \beta < 1$ and $C_{\mathrm{loc}} > 0$, independent of H, ℓ, and k, such that for any $v_H \in V_H$

$$\|(\mathcal{C}_\Phi - \mathcal{C}_\Phi^\ell)v_H\|_{1,k} \leq C_{\mathrm{loc}} \ell^{d/2} \beta^\ell \|v_H\|_{1,k}.$$

In the localized variant of the iterative multiscale approximation from Section 3.2, $\mathcal{C}_{u_H^m}$ is replaced by $\mathcal{C}_{u_H^m}^\ell$. As discussed, in this approach all localized element correctors $\mathcal{C}_{u_H^m,T}^\ell$ are newly computed in each step even if u_H^m has only slightly changed on the patch $\mathrm{N}^\ell(T)$. To introduce our adaptive approach, we need to estimate the error between element correction operators $\mathcal{C}_{\Phi,T}^\ell - \mathcal{C}_{\Psi,T}^\ell$ for two different functions $\Phi, \Psi \in H^1(D)$. In this setting, one should consider $\mathcal{C}_{\Psi,T}^\ell$ as being *available*, i.e., it has already been computed for instance in a previous iteration step, whereas $\mathcal{C}_{\Phi,T}^\ell$ is not available (only the function Φ). In our implementation, we use the following error indicator

$$(3.28) \quad E(\mathcal{C}_{\Phi,T}^\ell, \mathcal{C}_{\Psi,T}^\ell)^2 := \sum_{K \in \mathrm{N}^\ell(T)} \|n\varepsilon(|\Phi|^2 - |\Psi|^2)\|_{L^\infty(K)}^2 \max_{v|_T : v \in V_H} \frac{\|\chi_T v - \mathcal{C}_{\Psi,T}^\ell v\|_{0,K}^2}{\|v\|_{0,T}^2},$$

where χ_T denotes the indicator function for the element T. Note that the error indicator avoids the computation of $\mathcal{C}_{\Phi,T}^\ell$. We now have the following result.

Lemma 3.8. Let $\Phi, \Psi \in H^1(D)$ satisfy (2.7). Then, for any $v_H \in V_H$ it holds

$$(3.29) \qquad\qquad \|(\mathcal{C}_{\Phi,T}^\ell - \mathcal{C}_{\Psi,T}^\ell)v_H\|_{1,k} \leq \gamma^{-1} E(\mathcal{C}_{\Phi,T}^\ell, \mathcal{C}_{\Psi,T}^\ell) \|v_H\|_{1,k,T}$$

and there exists $C_{\mathrm{ol}} > 0$, independent of H, ℓ, and k, such that for any $v_H \in V_H$ it holds

$$(3.30) \qquad \|(\mathcal{C}_\Phi^\ell - \mathcal{C}_\Psi^\ell)v_H\|_{1,k} \leq C_{\mathrm{ol}} \ell^{d/2} \gamma^{-1} \big(\max_{T \in \mathcal{T}_H} E(\mathcal{C}_{\Phi,T}^\ell, \mathcal{C}_{\Psi,T}^\ell) \big) \|v_H\|_{1,k}.$$

The proof of this lemma and a detailed discussion of the error indicator are postponed to the appendix in order to ease the reading. We emphasize that the main result in Theorem 3.9 does not depend on the exact form of the error indicator, but only needs the estimates of Lemma 3.8.

Generalizing the setting of the previous section, we now define a sequence of adaptive multiscale solutions $\{\tilde{u}_H^m\}_{m \in \mathbb{N}}$ as outlined in Algorithm 1 below.

Algorithm 1 Adaptive iterative multiscale approximation

---

input: tolerance `tol`, starting value $\tilde{u}_H^0 \in V_H$, mesh $\mathcal{T}_H$, oversampling parameter ℓ

1: **for** $m = 1, 2, \ldots$ **do**
2:      **for all** $T \in \mathcal{T}_H$ **do**
3:          **if** $m = 1$ **then**
4:              $E_T^m \leftarrow \infty$
5:          **else**
6:              $E_T^m \leftarrow E(\mathcal{C}_{\tilde{u}_H^{m-1},T}^\ell, \tilde{\mathcal{C}}_{m-2,T}^\ell)$ ▷ does **not** explicitly require $\mathcal{C}_{\tilde{u}_H^{m-1},T}^\ell$
7:          **end if**

8:      **end for**
9:      $\mathcal{M}_m \leftarrow \{T \in \mathcal{T}_H : E_T^m > \texttt{tol}\}$ ▷ elements for which the corrector is updated
10:     **for all** $T \in \mathcal{T}_H$ **do**
11:        **if** $T \in \mathcal{M}_m$ **then**
12:           compute $\mathcal{C}^\ell_{\tilde{u}_H^{m-1},T}$ and $\mathcal{C}^{\ell,*}_{\tilde{u}_H^{m-1},T}$
13:           $\tilde{\mathcal{C}}^\ell_{m-1,T} \leftarrow \mathcal{C}^\ell_{\tilde{u}_H^{m-1},T}$ ▷ update corrector
14:        **else**
15:           $\tilde{\mathcal{C}}^\ell_{m-1,T} \leftarrow \mathcal{C}^\ell_{m-2,T}$ ▷ reuse the old corrector
16:        **end if**
17:        $\tilde{\mathcal{C}}^\ell_{m-1} \leftarrow \sum_{T \in \mathcal{T}_H} \tilde{\mathcal{C}}^\ell_{m-1,T}$
18:        $\tilde{\mathcal{C}}^{\ell,*}_{m-1} \leftarrow \sum_{T \in \mathcal{T}_H} \tilde{\mathcal{C}}^{\ell,*}_{m-1,T}$
19:     **end for**
20:     compute $\tilde{u}_H^m \in (1 - \tilde{\mathcal{C}}^\ell_{m-1})V_H$ as the solution of

$$(3.31) \qquad \mathcal{B}_{\mathrm{lin}}(\tilde{u}_H^{m-1}; \tilde{u}_H^m, v_H) = (f, \overline{v_H})$$

        for all $v_H \in (1 - \tilde{\mathcal{C}}^{\ell,*}_{m-1})V_H$
21: **end for**

output: sequence $\{\tilde{u}_H^m\}_{m \in \mathbb{N}}$

Let us shortly explain the adaptive algorithm. For $m = 1$, all correctors are computed based on the starting value $\tilde{u}_H^0$ and the LOD solution is computed as described in the previous section. In particular, if we choose the same starting value, we have $\tilde{u}_H^1 = u_H^1$ (up to the localization of the correctors). In the subsequent iterations, we decide, for each element T, whether to compute a new corrector based upon our error indicator E. Otherwise, the available corrector from the previous iteration(s) is used. Then, we assemble the LOD stiffness matrix using the mixture of newly computed and reused correctors and the previous LOD iterate $\tilde{u}_H^{m-1}$ for the nonlinearity. We emphasize that we do not reuse contributions to the stiffness matrix as suggested for lagging or perturbed linear diffusion problems in [HM19, HKM20]. In practice, the loop of the above algorithm will of course be terminated using the residual $\texttt{res}^m$ in the mth step as stopping criterion (together with a second tolerance $\texttt{TOL}$ as input). Let us also emphasize that the loop over all elements (lines 10 to 19) allows for parallel computations. Finally, we note that in the extreme cases $\texttt{tol} = 0$ or $\texttt{tol} = \infty$, we obtain the algorithm from Section 3.2 or a fixed-point iteration with fixed multiscale space $(1 - \mathcal{C}^\ell_{\tilde{u}_H^0})V_H$, respectively.

The well-posedness of (3.31) does not follow from Lemma 3.3 because not all element correctors are newly computed. However, the well-posedness of the algorithm as well as the a priori estimate for the error $\tilde{u}_H^m - u^m$ can be shown in a similar fashion as in Lemma 3.3 and Theorem 3.4. The additional errors by the localization and the adaptive update of the correctors are only small perturbations for sufficiently large ℓ and sufficiently small $\texttt{tol}$, cf. Lemma 3.7 and Lemma 3.8. More precisely, we have the following analog of Theorem 3.4. The proof with all technical details is again postponed to the appendix.

Theorem 3.9. *Assume that ℓ and $\texttt{tol}$ satisfy*

$$(3.32) \qquad \ell \gtrsim \left| \log\left(\frac{\delta(k)\gamma^2}{36\, C_\mathcal{B}^3 C_{\mathrm{int}}^3 C_{\mathrm{loc}}} \right) \right| / |\log(\beta)| \quad \textit{and} \quad \ell \gtrsim \left| \log\left(\frac{C_\mathcal{B}}{\gamma C_{\mathrm{loc}}} \right) \right| / |\log(\beta)|$$

as well as

$$(3.33) \qquad \texttt{tol} \leq \frac{\delta(k)\gamma^3}{36\, C_{\text{int}}^3 C_{\mathcal{B}}^3 C_{\text{ol}} \ell^{d/2}} \quad and \quad \texttt{tol} \leq \frac{C_{\mathcal{B}}}{C_{\text{ol}} \ell^{d/2}}.$$

Define $\hat{C}_{\text{stab}}(k) := \max\{C_{\text{stab}}, \frac{18\, C_{\text{int}}^2 C_{\mathcal{B}}^2}{\delta(k)\gamma^2}\}$ *with the constant* $C_{\text{stab}}(k)$ *from Proposition 2.4. Further, suppose that*

$$(3.34) \qquad 2\hat{C}_{\text{stab}}^3(k) C_n C_\varepsilon C_{\text{Nir}}^3 k^{d-1} \|f\|_0^2 \leq \vartheta.$$

Then the sequence $\{\tilde{u}_H^m\}_{m\in\mathbb{N}}$ *of adaptive iterative multiscale approximations is well-defined and satisfies the error estimate*

(3.35)
$$\|\tilde{u}_H^m - u^m\|_{1,k} \leq \vartheta^m \|\tilde{u}_H^0 - u^0\|_{1,k}$$
$$+ \frac{2}{1-\vartheta} \gamma^{-1} C_{\text{int}} \big(H + C_{\mathcal{B}} C_{\text{loc}}\, \ell^{d/2} \beta^\ell + C_{\mathcal{B}} C_{\text{stab}}(k) C_{\text{ol}}\, \ell^{d/2} \gamma^{-1} \texttt{tol}\big) \|f\|_0.$$

We emphasize that the first condition of (3.32) and (3.33), respectively, is the dominant condition. Condition (3.32) requires ℓ to grow with increasing wave numbers k. Under the assumption of polynomial stability, i.e., $C_{\text{stab},0} \approx k^q$ for some $q \geq 0$ and hence $\delta(k) \approx k^{-(q+1)}$, ℓ has to grow logarithmically in k as for the linear Helmholtz equation, see [GP15, Pet17, PV20]. The tolerance $\texttt{tol}$ has to decrease with growing k, in particular under the assumption of polynomial stability as before, we have $\texttt{tol} \lesssim k^{-(q+1)}$. We emphasize that this qualitative behavior is expected because for growing wave numbers, the nonlinearity becomes more dominant which has to be compensated by more updates of the correctors. The error between $\tilde{u}_H^m$ and u^m in the energy norm in (3.35) is essentially of order $H + \beta^\ell + \texttt{tol}$. The order $H + \beta^\ell$ occurs also in the study of the linear Helmholtz equation [GP15, Pet17, PV20] and suggests to choose $\ell \approx |\log(H)|$ to obtain a linear rate. The additional term $\texttt{tol}$ obviously comes from the reuse of correctors and can be made arbitrarily small at the price of growing computational costs.

In other words, as mentioned, for $\texttt{tol} = 0$ we obtain the localized version of the algorithm in Section 3.2. All additional terms and factors in Theorem 3.9 in comparison to Theorem 3.4 are caused by the handling of the additional localization error. We note that the factor 18 in $\hat{C}_{\text{stab}}(k)$ and the factor 3 in (3.35) can be made smaller for $\texttt{tol} = 0$ by a close inspection of the proof. In fact for zero tolerance, all steps where we switch between $\tilde{\mathcal{C}}_{m-1}^\ell$ and $\mathcal{C}_{\tilde{u}_H^{m-1}}^\ell$ can be omitted.

4. Numerical Examples

In this section, we present numerical examples to investigate the practical performance of our proposed iterative multiscale method. Note that in our studies the exact solution u of the nonlinear problem (2.2) is not explicitly known. Therefore, we compare the iterative multiscale solutions computed in (3.31) with a reference solution u_h, which is computed as a standard finite element approximation of (2.2). We implicitly assume that h is small enough such that u_h is a reasonable approximation of u. In particular, the mesh size h needs to resolve the multiscale features in the coefficients A, n, and ε. Further, we measure all errors in the energy norm $\|\cdot\|_{1,k}$.

We consider the domain $D = (0,1)^2$ and choose the fine mesh size $h = 2^{-9}$ and let the coefficients vary on a mesh $\mathcal{T}_\eta$ on the scale $\eta = 2^{-7}$. All numerical examples are computed with Python using an adapted version of the software $\texttt{gridlod}$ [HK19], which is based on
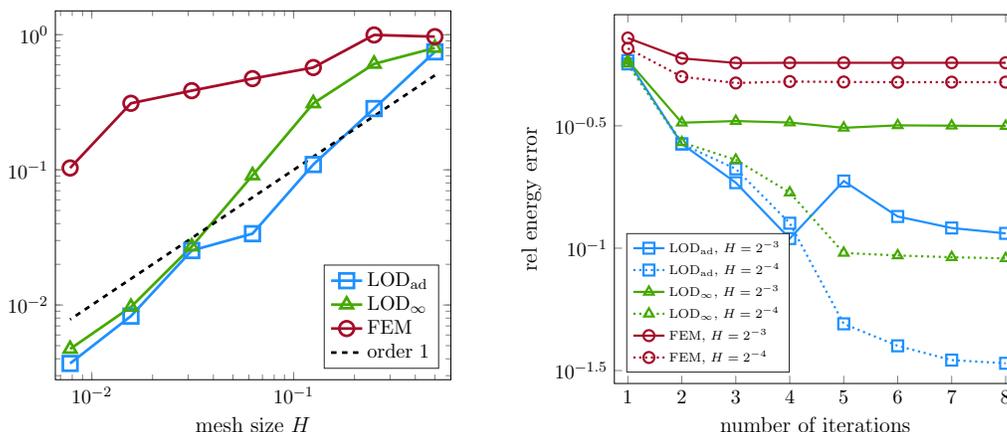
FIGURE 4.1. Relative energy errors of different iterative methods (left) and errors with respect to the number of iterations (right) for Example 1.

the Petrov-Galerkin version of the LOD method described above. The code is available at https://github.com/BarbaraV/gridlod-nonlinear-helmholtz.

4.1. **Example 1: point source.** For the first example, we consider the right-hand side

$$f(x) = \begin{cases} 10000 \exp\left(-\dfrac{1}{1 - \left(\frac{|x-x_0|}{0.05}\right)}\right) & \text{if } \frac{|x-x_0|}{0.05} < 1, \\ 0 & \text{else,} \end{cases}$$

with center $x_0 = (0.5, 0.5)$. Further, we have $k = 17$ and the domain where the nonlinearity is active is given by $D_\varepsilon = [0.55, 0.75] \times [0.25, 0.45]$. The scalar coefficients A, n, and ε are chosen as piecewise constant coefficients on the finite element mesh $\mathcal{T}_\eta$. More precisely, the values on each element are obtained as independent and uniformly distributed random numbers within the intervals $[0.5, 3]$, $[0.5, 1]$, and $[0, 9.4]$ for A, n, and ε, respectively.

We compute the reference solution on the mesh $\mathcal{T}_h$, as mentioned above, which is obtained by an iterative solution similarly as described in (2.12). Note that this discrete iteration is well-posed as pointed out in Remark 2.8. We iterate until the (relative) residual reaches the threshold of 10^{-12}, which requires 45 iterations.

In Figure 4.1 (left, □), we show the smallest errors of LOD solutions with $\ell = 2$ for different values of H within the first 20 iterations. For this particular example, we adapt the tolerance for the update of the correctors in each step. In particular, we only update element correctors whose error indicator (as defined in (3.28)) is larger than half the value of the maximal error indicator in this iteration. Note that, in the first iteration, all element correctors have to be computed. Afterwards, the maximal update percentages within the first 20 iterations for $H = 2^{-1}, 2^{-2}, 2^{-3}, 2^{-4}, 2^{-5}, 2^{-6}, 2^{-7}$ are 50, 6.25, 6.25, 3.52, 1.56, 0.88, 0.37 (in %), respectively. We emphasize that these percentages are with respect to the total number of elements in the corresponding mesh, which of course increases when H is decreased. In this example, the iterative method reaches a fixed point for all choices of H within the first 15 iterations. Further, the choice $\ell = 2$ shows to be sufficient, which is in line with the practical choices of ℓ in the linear case;
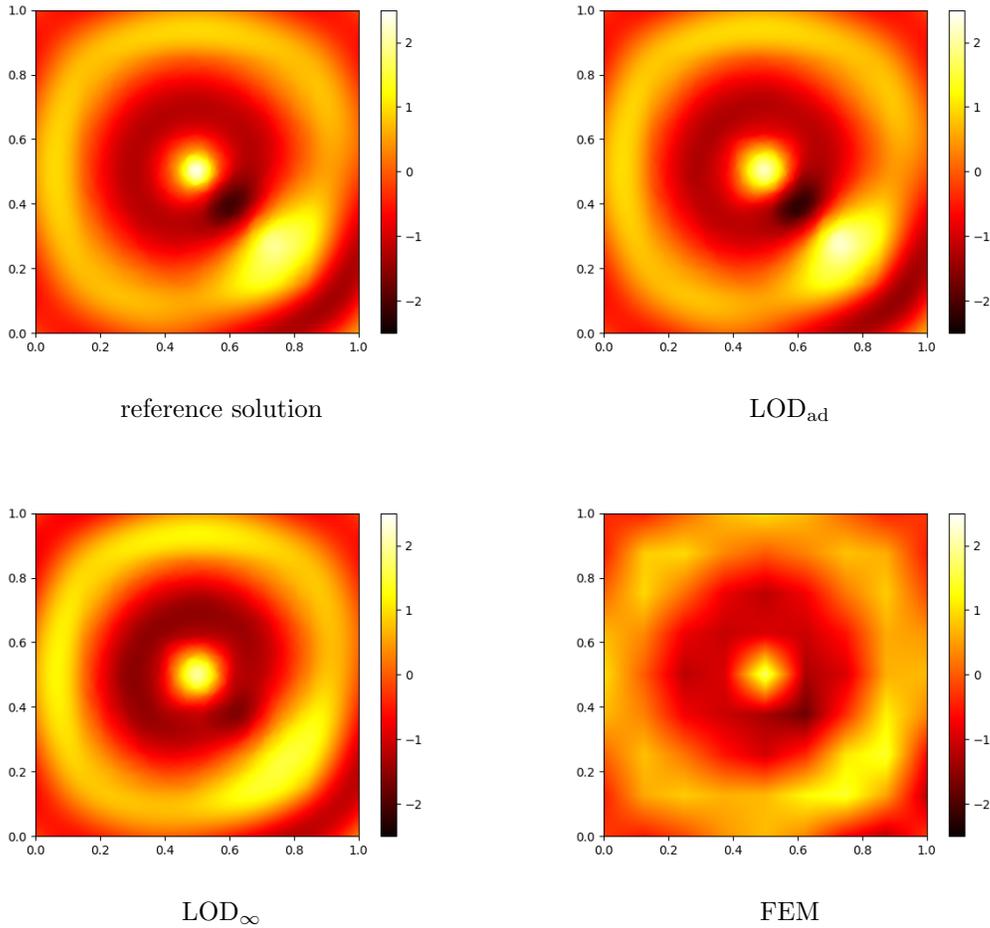
FIGURE 4.2. Real part of different final approximations on the scale $H = 2^{-3}$ and the corresponding reference solution for Example 1.

see, e.g. [BGP17, PV20]. Overall, the error shows a linear convergence rate underlining the findings of Theorem 3.9.

As comparison, we also present in Figure 4.1 (left) classical finite element approximations on the same scales H (○) as well as iterative LOD solutions for which the correctors are only computed in the first iteration and never updated afterwards (tol $= \infty$, △). The finite element approximation shows a suboptimal convergence rate and the error only improves when H is close to the scale η, i.e., where the coefficients are actually resolved by the coarse mesh. Then again, the LOD approximation which never updates the correctors starts off with a slow convergence similarly to the finite element approximation but heavily improves for smaller values of H, where the error is close to the one where the correctors are updated in every step. This behavior can be explained by the fact that the nonlinearity is only active in a small portion of the domain. Further, if H approaches η, the correctors become less influential. That is, for smaller values of H, very few updates of the correctors are already sufficient, which is also indicated by the small update percentages mentioned above.
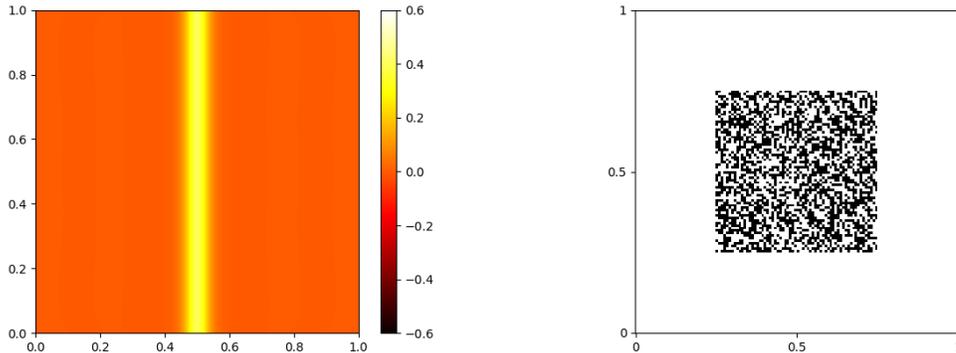
FIGURE 4.3. Real part of the incident beam u_{inc} (left) and Kerr coefficient with values 0 (white) and 0.85 (black) for Example 2.

The influence of the updates is especially important for larger values of H, see Figure 4.1 (right). There, we show the development of the relative errors of the different approximation methods for the particular cases $H = 2^{-3}$ (solid lines) and $H = 2^{-4}$ (dashed lines). The plot shows that the error significantly improves with the number of iterations provided that the correctors are (partially) updated. If the correctors are not updated after the first iteration, a faster stagnation can be observed. We note that the errors do not necessarily decrease monotonically, but this does not contradict our above theory.

Finally, we present in Figure 4.2 the final solutions for the three different approaches discussed above (LOD_{ad}, LOD_{∞}, and FEM) on the scale $H = 2^{-3}$ after 20 iterations as well as the reference solution. The figure shows that the LOD approximation with corrector updates leads to a very good approximation already on the relatively coarse scale $H = 2^{-3}$, while not updating the correctors after the first step deteriorates the behavior of the solution in the nonlinear domain. As expected, the finite element approximation, which does not take into account any variations of the coefficients, produces the worst result.

4.2. **Example 2: beam.** For the second example, we go beyond the above theory and consider an inhomogeneous boundary condition in (2.1), which is equivalent to adding a boundary source g. In particular, we choose the wave number $k = 30$ as well as the right-hand side f and the boundary term g that correspond to the incident beam

$$u_{\text{inc}}(x) = \frac{0.8 \exp(-\mathbf{i}k(0.5x_1 - 0.25))}{\cosh(50x_1 - 25) + 1},$$

which is illustrated in Figure 4.3 (left). More precisely, we take

$$f = -\Delta u_{\text{inc}} - k^2 u_{\text{inc}} \quad \text{in } D, \qquad g = \nabla u_{\text{inc}} \cdot \nu + \mathbf{i}k u_{\text{inc}} \quad \text{on } \Gamma.$$

As above, we choose A to be piecewise constant on the mesh $\mathcal{T}_\eta$, where values on each element are obtained as independent and uniformly distributed random numbers within the intervals $[0.2, 1]$. The Kerr coefficient is chosen as depicted in Figure 4.3 (right) with values 0 (white) and 0.85 (black), and $n \equiv 1$. Note that $D_\varepsilon = [0.25, 0.75]^2$ in this case. We again compute the corresponding reference solution iteratively on the mesh $\mathcal{T}_h$. The
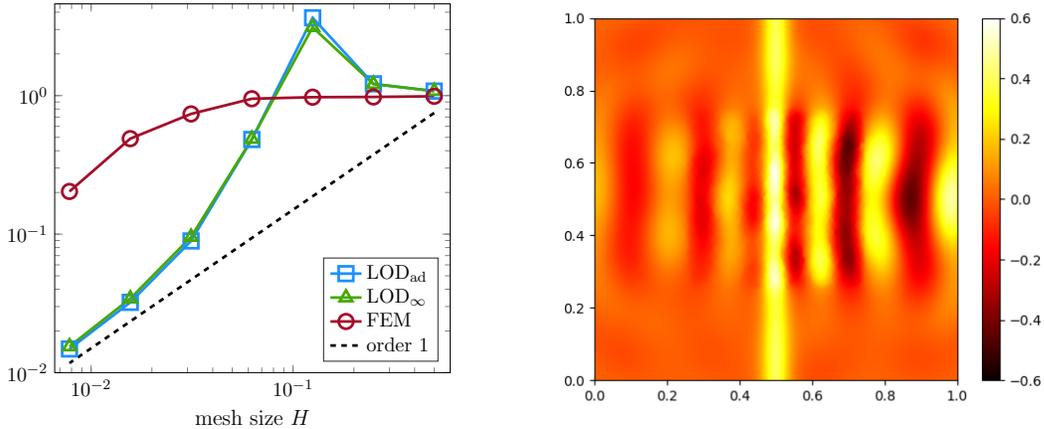
FIGURE 4.4. Relative energy errors of different iterative methods (left) and real part of the reference solution (right), both for Example 2.

threshold for the (relative) residual is again 10^{-12}, which is reached after 20 iterations. The reference solution is shown in Figure 4.4 (right) and shows scattering effects that appear due to the heterogeneity in A and the nonlinear Kerr term.

In Figure 4.4 (left) we present the smallest errors of LOD solutions with $\ell = 2$ for different values of H within the first 20 iterations. As above, we denote with LOD_{ad} ($\square$) the iterative method which only updates the element correctors whose error indicators are larger than 50% of the maximal value. Further, we show the errors for the iterative LOD solutions, where the correctors are only computed once (LOD_{∞}, $\triangle$) and a classical finite element approximation ($\bigcirc$). As above, we see a stagnation of the error curve of the finite element method if the scale of data oscillation is not resolved. Once the resolution condition $kH \lesssim 1$ is satisfied, both LOD curves show the predicted convergence and especially perform significantly better than the finite element approximation as expected. Note that the increase in the two LOD errors for the three first mesh sizes is caused by the violation of the resolution condition and, hence, does not contradict the above theory. In fact, we emphasize that similar peaks in the error curves are also observed for the linear Helmholtz equation if the resolution condition is not fulfilled, see [GP15, BGP17].

Finally, we emphasize that the two LOD curves with and without updates are very close in this example, since only very few iterations (≤ 4) are required to be close to a fixed point and the maximal values of the error indicator decrease heavily after the first iteration. The maximal update percentages, however, are higher than in the first example, which is related to D_ε being larger in the second one. These values are given by 100, 62.5, 12.5, 12.89, 6.93, 4.22, 1.07 (in %) for $H = 2^{-1}, 2^{-2}, 2^{-3}, 2^{-4}, 2^{-5}, 2^{-6}, 2^{-7}$.

5. CONCLUSION

Within this work, we proposed and analyzed an iterative multiscale method for a heterogeneous Helmholtz problem involving a Kerr-type nonlinearity. The method iteratively constructs (coarse) multiscale spaces that are partially updated in each iteration based on an appropriate error indicator. The approach allows for variations in the Kerr coefficient,

the refractive index, and the diffusion coefficient. We have proved well-posedness and convergence estimates of the method for arbitrarily rough coefficients under mild resolution conditions on the mesh size and appropriate bounds for the nonlinearity. In particular, we have quantified the influence of localization, linearization, and partial recalculations of multiscale spaces in each iteration. The presented numerical examples have confirmed the theoretical findings and in particular show that small updates in every iteration and moderate choices of the oversampling parameter are already sufficient to obtain reasonable approximations.

In general, adaptive iterative multiscale approximations open up a new perspective on the design of multiscale methods for nonlinear problems. In future research, this idea may be transferred to other types of problems such as, e.g., quasilinear diffusion-type problems or time-dependent quasilinear wave problems.

Acknowledgments

References

[AEEV12] A. Abdulle, W. E, B. Engquist, and E. Vanden-Eijnden. The heterogeneous multiscale method. *Acta Numer.*, 21:1–87, 2012.

[AH17] A. Abdulle and P. Henning. Localized orthogonal decomposition method for the wave equation with a continuum of scales. *Math. Comp.*, 86(304):549–587, 2017.

[AKS88] A. Kadir Aziz, R. B. Kellogg, and A. B. Stephens. A two point boundary value problem with a rapidly oscillating solution. *Numer. Math.*, 53(1-2):107–121, 1988.

[BFT09] G. Baruch, G. Fibich, and S. Tsynkov. A high-order numerical method for the nonlinear Helmholtz equation in multidimensional layered media. *J. Comput. Phys.*, 228(10):3789–3815, 2009.

[BGP17] D. Brown, D. Gallistl, and D. Peterseim. Multiscale Petrov-Galerkin method for high-frequency heterogeneous Helmholtz equations. In *Meshfree methods for partial differential equations VIII*, volume 115 of *Lect. Notes Comput. Sci. Eng.*, pages 85–115. Springer, Cham, 2017.

[BGT85] A. Bayliss, C. I. Goldstein, and E. Turkel. On accuracy conditions for the numerical computation of waves. *J. Comput. Phys.*, 59(3):396–404, 1985.

[Bre94] S. C. Brenner. Two-level additive Schwarz preconditioners for nonconforming finite elements. *Contemp. Math.*, 180:9–14, 1994.

[BS97] I. M. Babuška and S. A. Sauter. Is the pollution effect of the FEM avoidable for the Helmholtz equation considering high wave numbers? *SIAM J. Numer. Anal.*, 34(6):2392–2423, 1997.

[EE03] W. E and B. Engquist. The heterogeneous multiscale methods. *Commun. Math. Sci.*, 1(1):87–132, 2003.

[EE05] W. E and B. Engquist. The heterogeneous multi-scale method for homogenization problems. In *Multiscale methods in science and engineering*, volume 44 of *Lect. Notes Comput. Sci. Eng.*, pages 89–110. Springer, Berlin, Heidelberg, 2005.

[EG17] A. Ern and J.-L. Guermond. Finite element quasi-interpolation and best approximation. *ESAIM Math. Model. Numer. Anal.*, 51(4):1367–1385, 2017.

[EGH13] Y. Efendiev, J. Galvis, and T. Y. Hou. Generalized multiscale finite element methods (GMs-FEM). *J. Comput. Phys.*, 251:116–135, 2013.

[EH09] Y. Efendiev and T. Y. Hou. *Multiscale finite element methods*, volume 4 of *Surveys and Tutorials in the Applied Mathematical Sciences*. Springer, New York, 2009. Theory and applications.

[EW14]   G. Evéquoz and T. Weth. Real solutions to the nonlinear Helmholtz equation with local non-
            linearity. *Arch. Ration. Mech. Anal.*, 211(2):359–388, 2014.

[GG84]   J. A. Goldstone and E. Garmire. Intrinsic optical bistability in nonlinear media. *Phys. Rev.
            Lett.*, 53:910–913, 1984.

[GHV18]   D. Gallistl, P. Henning, and B. Verfürth. Numerical homogenization of H(curl)-problems. *SIAM
            J. Numer. Anal.*, 56(3):1570–1596, 2018.

[GP15]   D. Gallistl and D. Peterseim. Stable multiscale Petrov–Galerkin finite element method for high
            frequency acoustic scattering. *Comput. Methods Appl. Mech. Engrg.*, 295:1–17, 2015.

[GPS19]   I. G. Graham, O. R. Pembery, and E. A. Spence. The Helmholtz equation in heterogeneous
            media: a priori bounds, well-posedness, and resonances. *J. Differential Equations*, 266(6):2869–
            2923, 2019.

[Gri85]   P. Grisvard. *Elliptic problems in nonsmooth domains*, volume 24 of *Monographs and Studies in
            Mathematics*. Pitman, Boston, 1985.

[GS20]   I. G. Graham and S. A. Sauter. Stability and finite element error analysis for the Helmholtz
            equation with variable coefficients. *Math. Comp.*, 89(321):105–138, 2020.

[HK19]   F. Hellman and T. Keil. Gridlod. https://github.com/fredrikhellman/gridlod, 2019.
            GitHub repository, commit 0ed4c096df75040145978d48c5307ef5678efed3.

[HKM20]   F. Hellman, T. Keil, and A. Målqvist. Numerical upscaling of perturbed diffusion problems.
            SIAM J. Sci. Comput., 42(4):A2014–A2036, 2020.

[HM19]   F. Hellman and A. Målqvist. Numerical homogenization of elliptic PDEs with similar coeffi-
            cients. *Multiscale Model. Simul.*, 17(2):650–674, 2019.

[HMP14a]   P. Henning, A. Målqvist, and D. Peterseim. A localized orthogonal decomposition method for
            semi-linear elliptic problems. *ESAIM Math. Model. Numer. Anal.*, 48(05):1331–1349, 2014.

[HMP14b]   P. Henning, A. Målqvist, and D. Peterseim. Two-level discretization techniques for ground state
            computations of Bose-Einstein condensates. *SIAM J. Numer. Anal.*, 52(4):1525–1550, 2014.

[HP13]   P. Henning and D. Peterseim. Oversampling for the multiscale finite element method. *Multiscale
            Model. Simul.*, 11(4):1149–1175, 2013.

[HP20]   P. Henning and A. Persson. Computational homogenization of time-harmonic Maxwell's equa-
            tions. *SIAM J. Sci. Comput.*, 42(3):B581–B607, 2020.

[HW97]   T. Y. Hou and X.-H. Wu. A multiscale finite element method for elliptic problems in composite
            materials and porous media. *J. Comput. Phys.*, 134(1):169–189, 1997.

[JJWM08]   J. D. Joannapolous, S. G. Johnson, J. N. Winn, and R. D. Meade. *Photonic Crystals: Molding
            the Flow of Light*. Princeton University Press, Princeton, 2nd edition, 2008.

[Ker75]   J. Kerr. A new relation between electricity and light: Dielectrified media birefringent. *Philo-
            sophical Magazine*, 50:337–348, 1875.

[LSW20]   D. Lafontaine, E. A. Spence, and J. Wunsch. For most frequencies, strong trapping has a weak
            effect in frequency-domain scattering. *Commun. Pur. Appl. Math.*, published online:1–39, 2020.

[MP14]   A. Målqvist and D. Peterseim. Localization of elliptic multiscale problems. *Math. Comp.*,
            83(290):2583–2603, 2014.

[MP19]   R. Maier and D. Peterseim. Explicit computational wave propagation in micro-heterogeneous
            media. *BIT Numer. Math.*, 59(2):443–462, 2019.

[MS19]   A. Moiola and E. A. Spence. Acoustic transmission problems: wavenumber-explicit bounds and
            resonance-free regions. *Math. Models Methods Appl. Sci.*, 29(2):317–354, 2019.

[Nir59]   L. Nirenberg. On elliptic partial differential equations. *Ann. Scuola Norm. Sup. Pisa Cl. Sci.
            (3)*, 13:115–162, 1959.

[Osw93]   P. Oswald. On a BPX-preconditioner for P1 elements. *Computing*, 51(2):125–133, 1993.

[Pen00]   J. B. Pendry. Negative refraction makes a perfect lens. *Phys. Rev. Lett.*, 85(18):3966–3969,
            2000.

[Pet17]   D. Peterseim. Eliminating the pollution effect in Helmholtz problems by local subscale correc-
            tion. *Math. Comp.*, 86(305):1005–1036, 2017.

[PSS06]   J. B. Pendry, D. Schurig, and D. R. Smith. Controlling electromagnetic fields. *Science*,
            312(5781):1780–1782, 2006.

[PV20]   D. Peterseim and B. Verfürth. Computational high frequency scattering from high-contrast
            heterogeneous media. *Math. Comp.*, 89(326):2649–2674, 2020.

[PWW93] B. Proctor, E. Westwig, and F. Wise. Characterization of a Kerr-lens mode-locked Ti:sapphire laser with positive group-velocity dispersion. *Opt. Lett.*, 18:1654–1656, 1993.

[SPW04] D. R. Smith, J. B. Pendry, and M. C. K. Wiltshire. Metamaterials and negative refractive index. *Science*, 305(5685):788–792, 2004.

[ST18] S. A. Sauter and C. Torres. Stability estimate for the Helmholtz equation with rapidly jumping coefficients. *Z. Angew. Math. Phys.*, 69(6):Art. 139, 30, 2018.

[Ver17] B. Verfürth. Numerical homogenization for indefinite H(curl)-problems. In K. Mikula, D. Sevcovic, and J. Urban, editors, *Proceedings of Equadiff 2017 conference*, pages 137–146. Slovak University of Technology, Bratislava, 2017.

[Ver19] B. Verfürth. Numerical homogenization for nonlinear strongly monotone problems. *ArXiv Preprint*, 1907.01883, 2019.

[WZ18] H. Wu and J. Zou. Finite element method and its analysis for a nonlinear Helmholtz equation with high wave numbers. *SIAM J. Numer. Anal.*, 56(3):1338–1359, 2018.

[XB10] Z. Xu and G. Bao. A numerical scheme for nonlinear Helmholtz equations with strong nonlinear optical effects. *J. Opt. Soc. Am. A*, 27(11):2347–2353, 2010.

[YL17] L. Yuan and Y. Y. Lu. Robust iterative method for nonlinear Helmholtz equation. *J. Comput. Phys.*, 343:1–9, 2017.

Appendix A. Proofs of the results in Section 3.3

In this appendix, we prove Lemma 3.8 and Theorem 3.9. We use the same notation as in Section 3.3.

A.1. **Proof of Lemma 3.8.** Recall that $E(\mathcal{C}_{\Phi,T}^\ell, \mathcal{C}_{\Psi,T}^\ell)$ is an indicator in the sense that it yields an upper bound on the error $\mathcal{C}_{\Phi,T}^\ell - \mathcal{C}_{\Psi,T}^\ell$ without computing $\mathcal{C}_{\Phi,T}^\ell$ itself. The indicator consists of two main factors:

(i) the error in the nonlinear coefficient

$$\|n\varepsilon(|\Psi|^2 - |\Phi|^2)\|_{L^\infty(K)}$$

for which only Φ and Ψ themselves are required, but not the corresponding correctors and

(ii) the factor

$$\max_{v|_T : v \in V_H} \frac{\|\chi_T v - \mathcal{C}_{\Psi,T}^\ell v\|_{0,K}^2}{\|v\|_{0,T}^2}$$

which can be pre-computed when calculating $\mathcal{C}_{\Psi,T}^\ell$. This requires the solution of a small L^2-eigenvalue problem and in particular, the factor itself is a coarse-scale quantity so that the demanded storage is negligible.

We emphasize that in practice the functions Φ and Ψ in the error indicator will be iterative multiscale approximations and thus fully discrete objects. This justifies the use of the L^∞-norm here. Throughout the paper and especially in Section 2 we avoided the L^∞-norm because of the low regularity setting. One can also rewrite the error indicator and the proof below with the Nirenberg-type inequality such that it holds for general functions $\Phi, \Psi \in H^1(\Omega) \setminus L^\infty(\Omega)$. The rewritten error indicator involves L^3-norms in its two main factors analyzed above which we did not consider for implementational reasons.

Proof of Lemma 3.8. We abbreviate $z := (\mathcal{C}_{\Phi,T}^\ell - \mathcal{C}_{\Psi,T}^\ell)v_H$ and recall that $z \in \mathcal{W}(\mathrm{N}^\ell(T))$. Lemma 3.1 and (3.27) therefore yield

$$\gamma\|z\|_{1,k}^2 \le \mathcal{B}_{\mathrm{lin}}(\Phi; z, z) = \mathcal{B}_{\mathrm{lin},T}(\Phi; v_H, z) - \mathcal{B}_{\mathrm{lin},T}(\Psi; v_H, z)$$
$$+ \mathcal{B}_{\mathrm{lin},\mathrm{N}^\ell(T)}(\Psi; \mathcal{C}_{\Psi,T}^\ell v_H, z) - \mathcal{B}_{\mathrm{lin},\mathrm{N}^\ell(T)}(\Phi; \mathcal{C}_{\Psi,T}^\ell v_H, z)$$

$$\leq k\|n\varepsilon(|\Phi|^2 - |\Psi|^2)(\chi_T v_H - \mathcal{C}^\ell_{\Psi,T} v_H)\|_{0,\mathrm{N}^\ell(T)}\|z\|_{1,k}.$$

After dividing by $\|z\|_{1,k}$ and taking the square on both sides, we further obtain

$$\begin{aligned}
\gamma^2\|z\|_{1,k}^2 &\leq k^2\|n\varepsilon(|\Phi|^2 - |\Psi|^2)(\chi_T v_H - \mathcal{C}^\ell_{\Psi,T} v_H)\|_{0,\mathrm{N}^\ell(T)}^2 \\
&\leq \sum_{K\in\mathrm{N}^\ell(T)} k^2\|n\varepsilon(|\Phi|^2 - |\Psi|^2)\|_{L^\infty(K)}^2\|(\chi_T v_H - \mathcal{C}^\ell_{\Psi,T} v_H)\|_{0,K}^2 \\
&\leq \sum_{K\in\mathrm{N}^\ell(T)} \|n\varepsilon(|\Phi|^2 - |\Psi|^2)\|_{L^\infty(K)}^2 \Big(\max_{w|_T\,:\,w\in V_H} \frac{\|(\chi_T w - \mathcal{C}^\ell_{\Psi,T} w)\|_{0,K}^2}{\|w\|_{0,T}^2}\Big) k^2\|v_H\|_{0,T}^2 \\
&\leq E(\mathcal{C}^\ell_{\Phi,T}, \mathcal{C}^\ell_{\Psi,T})^2 \|v_H\|_{1,k,T}^2,
\end{aligned}$$

which shows (3.29).

Due to the definition of $\mathcal{C}^\ell_\Phi$ and $\mathcal{C}^\ell_\Psi$ as sums of element correctors with support only in $\mathrm{N}^\ell(T)$, we then deduce that there exists a constant C_{ol}, independent of H and ℓ such that

$$\begin{aligned}
\|(\mathcal{C}^\ell_\Phi - \mathcal{C}^\ell_\Psi)v_H\|_{1,k}^2 &\leq C_{\mathrm{ol}}^2 \ell^d \sum_{T\in\mathcal{T}_H} \|(\mathcal{C}^\ell_{\Phi,T} - \mathcal{C}^\ell_{\Psi,T})v_H\|_{1,k}^2 \\
&\leq C_{\mathrm{ol}}^2 \ell^d \gamma^{-2} \big(\max_{T\in\mathcal{T}_H} E(\mathcal{C}^\ell_{\Phi,T}, \mathcal{C}^\ell_{\Psi,T})\big)^2 \|v_H\|_{1,k}^2
\end{aligned}$$

and, hence, (3.30). $\qquad\square$

A.2. **Proof of Theorem 3.9.** Inspired by the proof of Theorem 3.4, we define for fixed $m \in \mathbb{N}$ an auxiliary solution $\tilde{w}^m \in H^1(D)$ as the solution of

$$(\mathrm{A.1}) \qquad\qquad \mathcal{B}_{\mathrm{lin}}(\tilde{u}_H^{m-1}; \tilde{w}^m, v) = (f, \overline{v})$$

for all $v \in H^1(D)$. The next proposition quantifies the error $\tilde{w}^m - \tilde{u}_H^m$. In particular, we first show that the LOD problem (3.31) in Algorithm 1 is well-posed. Note that this does not directly follow from Lemma 3.3 because not all element correctors are computed anew.

Proposition A.1. *Let $m \geq 1$ be fixed and let $\tilde{u}_H^{m-1}$ satisfy (2.7). Further, let $\delta(k)$ denote the inf-sup-constant with respect to $\mathcal{B}_{\mathrm{lin}}(\tilde{u}_H^{m-1}; \cdot, \cdot)$ in $H^1(D)$ as quantified in Lemma 3.2. Assume that (3.32) and (3.33) are fulfilled. Then, the following inf-sup-condition is satisfied,*

$$\inf_{v_H\in V_H} \sup_{w_H\in V_H} \frac{\Re\,\mathcal{B}_{\mathrm{lin}}(\tilde{u}_H^{m-1}; (1-\tilde{\mathcal{C}}^\ell_{m-1})v_H, (1-\tilde{\mathcal{C}}^{\ell,*}_{m-1})w_H)}{\|(1-\tilde{\mathcal{C}}^\ell_{m-1})v_H\|_{1,k}\,\|(1-\tilde{\mathcal{C}}^{\ell,*}_{m-1})w_H\|_{1,k}} \geq \frac{\delta(k)\gamma^2}{18C_{\mathrm{int}}^2 C_\mathcal{B}^2}.$$

In particular, $\tilde{u}_H^m$ is well-defined. Furthermore, we have

$$(\mathrm{A.2}) \quad \|\tilde{w}^m - \tilde{u}_H^m\|_{1,k} \leq 2\gamma^{-1}\,C_{\mathrm{int}}\big(H + C_\mathcal{B} C_{\mathrm{loc}}\,\ell^{d/2}\beta^\ell + C_\mathcal{B} C_{\mathrm{stab}}(k)C_{\mathrm{ol}}\,\ell^{d/2}\,\gamma^{-1}\,\mathtt{tol}\big)\|f\|_0.$$

Proof. Step 1 (inf-sup-constant): Let $v_H \in V_H$ be arbitrary but fixed. Due to the continuous inf-sup-condition (3.16), there exists $w \in H^1(D)$ with $\|w\|_{1,k} = 1$ such that

$$\Re\,\mathcal{B}_{\mathrm{lin}}(\tilde{u}_H^{m-1}; (1-\mathcal{C}_{\tilde{u}_H^{m-1}})v_H, w) \geq \delta(k)\,\|(1-\mathcal{C}_{\tilde{u}_H^{m-1}})v_H\|_{1,k}.$$

We set $w_H = \mathcal{I}_H w$ and deduce

$$
\begin{aligned}
\Re \mathcal{B}_{\mathrm{lin}}(\tilde{u}_H^{m-1}; (1 - \tilde{\mathcal{C}}_{m-1}^\ell)v_H, (1 - \tilde{\mathcal{C}}_{m-1}^{\ell,*})w_H) \\
= \Re \mathcal{B}_{\mathrm{lin}}(\tilde{u}_H^{m-1}; (1 - \mathcal{C}_{\tilde{u}_H^{m-1}}^\ell)v_H, (1 - \tilde{\mathcal{C}}_{m-1}^{\ell,*})w_H) \\
- \Re \mathcal{B}_{\mathrm{lin}}(\tilde{u}_H^{m-1}; (\tilde{\mathcal{C}}_{m-1}^\ell - \mathcal{C}_{\tilde{u}_H^{m-1}}^\ell)v_H, (1 - \tilde{\mathcal{C}}_{m-1}^{\ell,*})w_H) \\
= \Re \mathcal{B}_{\mathrm{lin}}(\tilde{u}_H^{m-1}; (1 - \mathcal{C}_{\tilde{u}_H^{m-1}})v_H, (1 - \tilde{\mathcal{C}}_{m-1}^{\ell,*})w_H) \\
- \Re \mathcal{B}_{\mathrm{lin}}(\tilde{u}_H^{m-1}; (\mathcal{C}_{\tilde{u}_H^{m-1}}^\ell - \mathcal{C}_{\tilde{u}_H^{m-1}})v_H, (1 - \tilde{\mathcal{C}}_{m-1}^{\ell,*})w_H) \\
- \Re \mathcal{B}_{\mathrm{lin}}(\tilde{u}_H^{m-1}; (\tilde{\mathcal{C}}_{m-1}^\ell - \mathcal{C}_{\tilde{u}_H^{m-1}}^\ell)v_H, (1 - \tilde{\mathcal{C}}_{m-1}^{\ell,*})w_H) \\
= \Re \mathcal{B}_{\mathrm{lin}}(\tilde{u}_H^{m-1}; (1 - \mathcal{C}_{\tilde{u}_H^{m-1}})v_H, w) \\
- \Re \mathcal{B}_{\mathrm{lin}}(\tilde{u}_H^{m-1}; (\mathcal{C}_{\tilde{u}_H^{m-1}}^\ell - \mathcal{C}_{\tilde{u}_H^{m-1}})v_H, (1 - \tilde{\mathcal{C}}_{m-1}^{\ell,*})w_H) \\
- \Re \mathcal{B}_{\mathrm{lin}}(\tilde{u}_H^{m-1}; (\tilde{\mathcal{C}}_{m-1}^\ell - \mathcal{C}_{\tilde{u}_H^{m-1}}^\ell)v_H, (1 - \tilde{\mathcal{C}}_{m-1}^{\ell,*})w_H).
\end{aligned}
\tag{A.3}
$$

For the last equality, we wrote $1 - \tilde{\mathcal{C}}_{m-1}^{\ell,*} = 1 - \tilde{\mathcal{C}}_{m-1}^* + \tilde{\mathcal{C}}_{m-1}^* - \tilde{\mathcal{C}}_{m-1}^{\ell,*}$ and used the orthogonality of $(1 - \mathcal{C}_{\tilde{u}_H^{m-1}})V_H$ and $\mathcal{W}$ as well as $(1 - \tilde{\mathcal{C}}_{m-1}^*)\mathcal{I}_H w = (1 - \tilde{\mathcal{C}}_{m-1}^*)w$. Here, $\tilde{\mathcal{C}}_{m-1}$ is defined as $\tilde{\mathcal{C}}_{m-1}^\ell$ with $\ell = \infty$, i.e., on global patches. We can now use (A.3), the continuous inf-sup-condition (3.16), and the continuity of $\mathcal{B}_{\mathrm{lin}}$ to obtain

$$
\begin{aligned}
\Re \mathcal{B}_{\mathrm{lin}}(\tilde{u}_H^{m-1}; (1 - \tilde{\mathcal{C}}_{m-1}^\ell)v_H, (1 - \tilde{\mathcal{C}}_{m-1}^{\ell,*})w_H) \\
\geq \delta(k)\|(1 - \mathcal{C}_{\tilde{u}_H^{m-1}})v_H\|_{1,k} - C_{\mathcal{B}}\|(\mathcal{C}_{\tilde{u}_H^{m-1}}^\ell - \mathcal{C}_{\tilde{u}_H^{m-1}})v_H\|_{1,k}\|(1 - \tilde{\mathcal{C}}_{m-1}^{\ell,*})w_H\|_{1,k} \\
- C_{\mathcal{B}}\|(\tilde{\mathcal{C}}_{m-1}^\ell - \mathcal{C}_{\tilde{u}_H^{m-1}}^\ell)v_H\|_{1,k}\|(1 - \tilde{\mathcal{C}}_{m-1}^{\ell,*})w_H\|_{1,k}.
\end{aligned}
\tag{A.4}
$$

Lemma 3.7 yields

$$
\|(\mathcal{C}_{\tilde{u}_H^{m-1}}^\ell - \mathcal{C}_{\tilde{u}_H^{m-1}})v_H\|_{1,k} \leq C_{\mathrm{loc}}\ell^{d/2}\beta^\ell\|v_H\|_{1,k}.
\tag{A.5}
$$

Note that the adaptive algorithm ensures together with Lemma 3.8 that

$$
\|(\tilde{\mathcal{C}}_{m-1}^\ell - \mathcal{C}_{\tilde{u}_H^{m-1}}^\ell)v_H\|_{1,k}^2 \leq C_{\mathrm{ol}}^2 \ell^d \gamma^{-2} \mathtt{tol}^2\|v_H\|_{1,k}^2.
\tag{A.6}
$$

Furthermore, we have norm equivalences

$$
\begin{aligned}
\|v_H\|_{1,k} = \|\mathcal{I}_H((1 - \mathcal{C}_{\tilde{u}_H^{m-1}})v_H)\|_{1,k} \leq C_{\mathrm{int}}\|(1 - \mathcal{C}_{\tilde{u}_H^{m-1}})v_H\|_{1,k}, \\
\|v_H\|_{1,k} = \|\mathcal{I}_H((1 - \tilde{\mathcal{C}}_{m-1}^\ell)v_H)\|_{1,k} \leq C_{\mathrm{int}}\|(1 - \tilde{\mathcal{C}}_{m-1}^\ell)v_H\|_{1,k},
\end{aligned}
$$

as well as the estimate

$$
\begin{aligned}
\|(1 - \tilde{\mathcal{C}}_{m-1}^\ell)v_H\|_{1,k} \\
\leq \|(1 - \mathcal{C}_{\tilde{u}_H^{m-1}})v_H\|_{1,k} + \|(\mathcal{C}_{\tilde{u}_H^{m-1}} - \mathcal{C}_{\tilde{u}_H^{m-1}}^\ell)v_H\|_{1,k} + \|(\mathcal{C}_{\tilde{u}_H^{m-1}}^\ell - \tilde{\mathcal{C}}_{m-1}^\ell)v_H\|_{1,k} \\
\leq (\gamma^{-1}C_{\mathcal{B}} + C_{\mathrm{loc}}\ell^{d/2}\beta^\ell + C_{\mathrm{ol}}\ell^{d/2}\gamma^{-1}\mathtt{tol})\|v_H\|_{1,k} \\
\leq 3\gamma^{-1}C_{\mathcal{B}}\|v_H\|_{1,k},
\end{aligned}
$$

where we have used (3.32) and (3.33) in the last step. With the same line of arguments we can also show that

$$
\|(1 - \tilde{\mathcal{C}}_{m-1}^{\ell,*})w_H\|_{1,k} \leq 3\gamma^{-1}C_{\mathcal{B}}\|w_H\|_{1,k} \leq 3\gamma^{-1}C_{\mathcal{B}}C_{\mathrm{int}}\|w\|_{1,k}.
$$

Inserting (A.5)–(A.6) and these norm equivalences into (A.4), we finally obtain

$$\Re\, \mathcal{B}_{\mathrm{lin}}(\tilde{u}_H^{m-1}; (1-\tilde{\mathcal{C}}_{m-1}^\ell)v_H, (1-\tilde{\mathcal{C}}_{m-1}^{\ell,*})w_H)$$
$$\geq \Big(\delta(k)\frac{\gamma^2}{9C_{\mathcal{B}}^2 C_{\mathrm{int}}^2} - C_{\mathcal{B}}C_{\mathrm{int}}C_{\mathrm{loc}}\,\ell^{d/2}\beta^\ell - C_{\mathcal{B}}C_{\mathrm{int}}C_{\mathrm{ol}}\,\ell^{d/2}\,\gamma^{-1}\,\mathtt{tol}\Big)$$
$$\cdot \|(1-\tilde{\mathcal{C}}_{m-1}^\ell)v_H\|_{1,k}\|(1-\tilde{\mathcal{C}}_{m-1}^{\ell,*})w_H\|_{1,k},$$

which finishes the proof of the inf-sup-condition using the conditions (3.32)–(3.33).

   Step 2 (error estimate): We write $\tilde{u}_H^m = (1-\tilde{\mathcal{C}}_{m-1}^\ell)\mathcal{I}_H\tilde{u}_H^m$ and set $e := \tilde{w}^m - \tilde{u}_H^m$, where $\tilde{w}^m$ is the auxiliary solution defined in (A.1). Further, let $e_H^\ell := (1-\tilde{\mathcal{C}}_{m-1}^\ell)\mathcal{I}_H e$. Here, $\tilde{\mathcal{C}}_{m-1}$ is the corrector with $\ell = \infty$ as explained above. Observe that $e - e_H^\ell = \tilde{w}^m - (1-\tilde{\mathcal{C}}_{m-1}^\ell)\mathcal{I}_H\tilde{w}^m \in \mathcal{W}$. With Lemma 3.1, (3.4), (A.5), (A.6), and (2.8), we obtain
(A.7)
$$\gamma\,\|e-e_H^\ell\|_{1,k}^2 \leq \Re\,\mathcal{B}_{\mathrm{lin}}(\tilde{u}_H^{m-1}; \tilde{w}^m - (1-\tilde{\mathcal{C}}_{m-1}^\ell)\mathcal{I}_H\tilde{w}^m, e-e_H^\ell)$$
$$= \Re\,(f, \overline{e-e_H^\ell}) - \Re\,\mathcal{B}_{\mathrm{lin}}(\tilde{u}_H^{m-1}; (1-\mathcal{C}_{\tilde{u}_H^{m-1}}^\ell)\mathcal{I}_H\tilde{w}^m, e-e_H^\ell)$$
$$- \Re\,\mathcal{B}_{\mathrm{lin}}(\tilde{u}_H^{m-1}; (\mathcal{C}_{\tilde{u}_H^{m-1}}^\ell - \tilde{\mathcal{C}}_{m-1}^\ell)\mathcal{I}_H\tilde{w}^m, e-e_H)$$
$$= \Re\,(f, \overline{e-e_H^\ell}) - \Re\,\mathcal{B}_{\mathrm{lin}}(\tilde{u}_H^{m-1}; (\mathcal{C}_{\tilde{u}_H^{m-1}} - \mathcal{C}_{\tilde{u}_H^{m-1}}^\ell)\mathcal{I}_H\tilde{w}^m, e-e_H^\ell)$$
$$- \Re\,\mathcal{B}_{\mathrm{lin}}(\tilde{u}_H^{m-1}; (\mathcal{C}_{\tilde{u}_H^{m-1}}^\ell - \tilde{\mathcal{C}}_{m-1}^\ell)\mathcal{I}_H\tilde{w}^m, e-e_H)$$
$$\leq C_{\mathrm{int}}\big(H + C_{\mathcal{B}}C_{\mathrm{loc}}\ell^{d/2}\beta^\ell + C_{\mathcal{B}}C_{\mathrm{stab}}(k)C_{\mathrm{ol}}\,\ell^{d/2}\,\gamma^{-1}\,\mathtt{tol}\big)\|f\|_0\,\|e-e_H^\ell\|_{1,k}.$$

From the definitions of $\tilde{w}^m$ and $\tilde{u}_H^m$, we deduce the following Galerkin orthogonality

$$\mathcal{B}_{\mathrm{lin}}(\tilde{u}_H^{m-1}; e, w_H) = 0$$

for all $w_H \in (1-\tilde{\mathcal{C}}_{m-1}^{\ell,*})V_H$. Let $z_H^\ell \in (1-\tilde{\mathcal{C}}_{m-1}^{\ell,*})V_H$ be the unique solution of the dual problem

$$\mathcal{B}_{\mathrm{lin}}(\tilde{u}_H^{m-1}; v_H, z_H^\ell) = (v_H, \overline{e_H^\ell})_{1,k}$$

for all $v_H \in (1-\tilde{\mathcal{C}}_{m-1}^\ell)V_H$, which is well-posed by the inf-sup-condition that we have proved in step 1. We observe that $z_H^\ell = (1-\tilde{\mathcal{C}}_{m-1}^{\ell,*})\mathcal{I}_H z_H^\ell$. Due to the form of e_H^ℓ and the Galerkin orthogonality, we hence deduce

$$\|e_H^\ell\|_{1,k}^2 = \mathcal{B}_{\mathrm{lin}}(\tilde{u}_H^{m-1}; e_H^\ell, z_H^\ell)$$
$$= \mathcal{B}_{\mathrm{lin}}(\tilde{u}_H^{m-1}; e_H^\ell - e, z_H^\ell)$$
$$= \mathcal{B}_{\mathrm{lin}}(\tilde{u}_H^{m-1}; e_H^\ell - e, (1-\mathcal{C}_{\tilde{u}_H^{m-1}}^{\ell,*})\mathcal{I}_H z_H^\ell) + \mathcal{B}_{\mathrm{lin}}(\tilde{u}_H^{m-1}; e_H^\ell - e, (\mathcal{C}_{\tilde{u}_H^{m-1}}^{\ell,*} - \tilde{\mathcal{C}}_{m-1}^{\ell,*})\mathcal{I}_H z_H^\ell)$$
$$= \mathcal{B}_{\mathrm{lin}}(\tilde{u}_H^{m-1}; e_H^\ell - e, (\mathcal{C}_{\tilde{u}_H^{m-1}}^* - \mathcal{C}_{\tilde{u}_H^{m-1}}^{\ell,*})\mathcal{I}_H z_H^\ell)$$
$$+ \mathcal{B}_{\mathrm{lin}}(\tilde{u}_H^{m-1}; e_H^\ell - e, (\mathcal{C}_{\tilde{u}_H^{m-1}}^{\ell,*} - \tilde{\mathcal{C}}_{m-1}^{\ell,*})\mathcal{I}_H z_H^\ell)$$
$$\leq C_{\mathcal{B}}\,C_{\mathrm{int}}(C_{\mathrm{loc}}\,\ell^{d/2}\beta^\ell + C_{\mathrm{ol}}\ell^{d/2}\,\gamma^{-1}\,\mathtt{tol})\,\|z_H^\ell\|_{1,k}\,\|e_H^\ell - e\|_{1,k}$$
$$\leq C_{\mathcal{B}}\,C_{\mathrm{int}}\,(C_{\mathrm{loc}}\,\ell^{d/2}\beta^\ell + C_{\mathrm{ol}}\ell^{d/2}\,\gamma^{-1}\,\mathtt{tol})\,\frac{18C_{\mathrm{int}}^2 C_{\mathcal{B}}^2}{\delta(k)\gamma^2}\,\|e_H^\ell\|_{1,k}\,\|e_H^\ell - e\|_{1,k}.$$

Using the condition (3.32) on ℓ and (3.33), we obtain

$$\|e_H^\ell\|_{1,k} \leq \|e_H^\ell - e\|_{1,k}.$$

Together with (A.7) and an application of the triangle inequality, this concludes the proof. $\qquad\square$

This Proposition is now used inductively to prove Theorem 3.9.

Proof of Theorem 3.9. We proceed similarly as in the proof of Theorem 3.4. Let $m \geq 1$ be fixed and define the auxiliary solution $\tilde{w}^m \in H^1(D)$ as the solution of (A.1). Note that due to (3.34) and by Proposition 2.4 (as well as its adapted version for the series of multiscale solutions), we have the following stability estimates,

$$\|\tilde{u}_H^{m-1}\|_{1,k} \leq \frac{18\, C_{\text{int}}^2 C_{\mathcal{B}}^2}{\delta(k)\gamma^2} \|f\|_0,$$
$$\|u^m\|_{1,k} \leq C_{\text{stab}}(k)\, \|f\|_0,$$
$$\|\tilde{w}^m\|_{1,k} \leq C_{\text{stab}}(k)\, \|f\|_0.$$

Further, the error $e^m = u^m - \tilde{w}^m$ solves

$$\begin{aligned}
\mathcal{B}_{\text{lin}}(u^{m-1}; e^m, v) &= \mathcal{B}_{\text{lin}}(\tilde{u}_H^{m-1}; w^m, v) - \mathcal{B}_{\text{lin}}(u^{m-1}; w^m, v) \\
&= (k^2\varepsilon \mathbb{1}_{D_\varepsilon}(|u^{m-1}|^2 - |\tilde{u}_H^{m-1}|^2)w^m, \overline{v})
\end{aligned}$$

for all $v \in H^1(D)$. As in the proof of Theorem 3.4, we obtain

$$\|e^m\|_{1,k} \leq \vartheta\, \|\tilde{u}_H^{m-1} - u^{m-1}\|_{1,k}.$$

Combining this with Proposition A.1, we deduce

$$\begin{aligned}
\|\tilde{u}_H^m - u^m\|_{1,k} &\leq \vartheta\|\tilde{u}_H^{m-1} - u^{m-1}\|_{1,k} \\
&\quad + 2\gamma^{-1}C_{\text{int}}\big(H + C_{\mathcal{B}}C_{\text{loc}}\,\ell^{d/2}\beta^\ell + C_{\mathcal{B}}C_{\text{stab}}(k)C_{\text{ol}}\,\ell^{d/2}\,\gamma^{-1}\,\texttt{tol}\big)\|f\|_0 \\
&\leq \vartheta^m\|\tilde{u}_H^0 - u^0\|_{1,k} \\
&\quad + 2\gamma^{-1}C_{\text{int}}\big(H + C_{\text{loc}}C_{\mathcal{B}}\,\ell^{d/2}\beta^\ell + C_{\mathcal{B}}C_{\text{stab}}(k)C_{\text{ol}}\,\ell^{d/2}\,\gamma^{-1}\,\texttt{tol}\big)\|f\|_0 \sum_{n\in\mathbb{N}}\vartheta^n \\
&\leq \vartheta^m\|\tilde{u}_H^0 - u^0\|_{1,k} \\
&\quad + \frac{2}{1-\vartheta}\gamma^{-1}C_{\text{int}}\big(H + C_{\mathcal{B}}C_{\text{loc}}\,\ell^{d/2}\beta^\ell + C_{\mathcal{B}}C_{\text{stab}}(k)C_{\text{ol}}\,\ell^{d/2}\,\gamma^{-1}\,\texttt{tol}\big)\|f\|_0,
\end{aligned}$$

which concludes the proof. $\qquad\square$

† DEPARTMENT OF MATHEMATICAL SCIENCES, CHALMERS UNIVERSITY OF TECHNOLOGY AND UNIVERSITY OF GOTHENBURG, 412 96 GÖTEBORG, SWEDEN
E-mail address: roland.maier@chalmers.se

‡ INSTITUT FÜR ANGEWANDTE UND NUMERISCHE MATHEMATIK, KARLSRUHER INSTITUT FÜR TECHNOLOGIE, ENGLERSTR. 2, 76131 KARLSRUHE
E-mail address: barbara.verfuerth@kit.edu